SYNTHESIS, MIGRATION, AND RELEASE OF PRECURSOR COLLAGEN BY ODONTOBLASTS AS VISUALIZED BY RADIOAUTOGRAPHY AFTER [^{3}H]PROLINE ADMINISTRATION

MELVYN WEINSTOCK and C. P. LEBLOND

From the Department of Anatomy, McGill University, Montreal, Quebec, Canada

ABSTRACT

The elaboration of dentin collagen precursors by the odontoblasts in the incisor teeth of 30–40-g rats was investigated by electron microscopy, histochemistry, and radioautography after intravenous injection of tritium-labeled proline.

At 2 min after injection, when the labeling of blood proline was high, radioactivity was restricted to the rough endoplasmic reticulum, indicating that it is the site of synthesis of the polypeptide precursors of collagen, the pro-alpha chains.

At 10 min, when the labeling of blood proline had already declined, radioactivity was observed in spherical portions of Golgi saccules containing entangled threads, and, at 20 min, radioactivity appeared in cylindrical portions containing aggregates of parallel threads. The parallel threads measured 280–350 nm in length and stained with the low pH-phosphotungstic acid technique for carbohydrate and with the silver methenamine technique for aldehydes (as did extracellular collagen fibrils). The passage of label from spherical to cylindrical Golgi portions is associated with the reorganization of entangled into parallel threads, which is interpreted as the packing of procollagen molecules.

Between 20 and 30 min, prosecretory and secretory granules respectively became labeled. These results indicate that the cylindrical portions of Golgi saccules transform into prosecretory and subsequently into secretory granules. Within these granules, the parallel threads, believed to be procollagen molecules, are transported to the odontoblast process.

At 90 min and 4 h after injection, label was present in predentin, indicating that the labeled content of secretory granules had been released into predentin. This occurred by exocytosis as evidenced by the presence of secretory granules in fusion with the plasmalemma of the odontoblast process.

It is proposed that pro-alpha chains give rise to procollagen molecules which assemble into parallel aggregates in the Golgi apparatus. Procollagen molecules are then transported within secretory granules to the odontoblast process and released by exocytosis. In predentin procollagen molecules would give rise to tropocollagen molecules, which would then polymerize into collagen fibrils.

INTRODUCTION

Collagen is an extracellular fibrous protein that constitutes a major portion of connective tissue matrices, particularly the matrix of dentin (6, 15, 62). There is agreement that the polypeptide chains of collagen are assembled from amino acids on ribosomes (10, 21, 48); however, the intracellular pathway for collagen or its precursors prior to the appearance of individual fibrils in the extracellular matrix remains controversial. Several intracellular routes for collagen secretion have been proposed, mainly on the strength of radioautographic evidence. Studies on the fibroblast (57) led to the conclusion that collagen precursors may pass directly from the cisternae of the rough endoplasmic reticulum to the cell surface by intermittent fusion of the cisternal membrane with the plasma membrane or by small vesicles arising from the cisternae (20, 57). In the chondroblast and odontoblast, it has been proposed that collagen precursors pass from ribosomes into the cytoplasmic ground substance and subsequently through the plasma membrane to the cell surface (12, 53, 59). From their studies on the chondrocyte, Revel and Hay (55) asserted that collagen precursors are routed through the Golgi apparatus prior to their extracellular discharge. A similar pathway has been reported in the case of the osteoblast and odontoblast (16, 17).

From previous studies employing [^{3}H]glycine and [^{3}H]proline to trace collagen formation (8, 35), it was noted that odontoblasts in the continually erupting mouse incisor are actively engaged in collagen synthesis and that the collagen formed is secreted from a predictable location, the cell apex. This finding indicated that odontoblasts are among the most polarized cell types which produce collagen and, therefore, could be used to advantage to trace the intracellular migration of newly synthesized collagen.

In the present investigation, morphological, radioautographic, and histochemical methods have been employed in an attempt to identify the pathway of secretion for collagen precursors within the odontoblasts of the maxillary incisor tooth of the rat. In addition, since recent studies have shown that collagen is assembled in a series of sequential steps (22) which include synthesis of polypeptide chains, triple helix formation, glycosylation, and conversion to tropocollagen, the aim of the present study has also been to identify the intracellular sites where these steps occur in the odontoblast.

MATERIALS AND METHODS

Tissue Preparation

Under ether anaesthesia, male Sherman rats weighing 35–40 g each were sacrificed by intracardiac perfusion with solutions of either paraformaldehyde or glutaraldehyde. Tracheal intubation was carried out prior to perfusion with a polyethylene catheter (Venocath-18, no. 4816, Abbott Laboratories, Chicago, Ill.) connected to a tube providing either a 95% O_2 + 5% CO_2 mixture or ether vapors to control oxygenation and depth of anesthesia after surgical access to the thoracic cavity. For radioautographic experiments, perfusion was carried out at room temperature with a solution containing 3.0% formaldehyde (prepared from paraformaldehyde, Taab Laboratories, Emmer Green, Reading, England, according to the method of Karnovsky [29]), 0.1 M Sörensen's phosphate buffer, and 0.1% sucrose. The osmolality was 1,150 M osmol and the pH was 7.3. For morphological studies, the perfusate consisted of 2.5% glutaraldehyde (Taab Laboratories) in 0.05 M Sörensen's phosphate buffer (pH 7.3) with the addition of 0.1% sucrose and 0.5% dextrose (400 M osmol). In both cases, the fixative solution was administered through the left ventricle by means of a cooled polyethylene catheter (Venocath-16) attached to a Ministatic pump (Manostat Corp., New York) set at a reading of 0.3. After 10 min the pump was turned off and the fixative allowed to flow by gravity for an additional 10 min.

The maxillae were removed, immersed for an additional 3–4 h in fresh fixative of the type initially used and demineralized for 2 wk at 4°C in EDTA (70). In the case of formaldehyde-fixed tissues, 0.11 M sucrose was added to the EDTA; demineralization was followed by an overnight rinse in 0.1 M Sörensen's phosphate buffer, pH 7.3, containing 0.22 M sucrose. For glutaraldehyde-fixed tissues, sucrose was omitted from the EDTA and the buffer rinse consisted of 0.15 M Sörensen's phosphate buffer.

The maxillae, each containing one incisor tooth, were then sliced transversely into 1-mm thick sections and immersed in 1% osmium tetroxide buffered with 0.1 M Sörensen's phosphate for 1/2 h. Specimens were dehydrated in a graded series of acetone at room temperature and embedded in Epon.

For light microscopy, semithin 0.5-μm sections were mounted on glass slides and stained with 1% toluidine blue in a saturated borax solution. For

electron microscopy, thin sections with silver to gold interference colors were mounted on copper grids and stained either with saturated aqueous uranyl acetate plus lead citrate or with lead citrate alone (56, 67) and examined in a Siemens Elmiskop I or 101.

Histochemistry

STAINING WITH SILVER METHENAMINE: Ultrathin sections of glutaraldehyde-fixed tissue were mounted on 400-mesh nickel grids and stained with silver methenamine (42).

DETECTION OF GLYCOPROTEIN: Glutaraldehyde-fixed incisor teeth were embedded in glycol methacrylate (37). Thin sections were floated for 30 min to 1 h on a freshly prepared, filtered solution of 1% phosphotungstic acid in 1 N HCl (52), rinsed very briefly in distilled water, and transferred to copper grids.

Radioautography

[^{3}H]PROLINE ADMINISTRATION: Under ether anaesthesia, each animal received by way of the external jugular vein a slow injection of 0.2 ml of 0.05 N HCl containing 2.5 mCi of L-[2,3-^{3}H]proline (45.7 Ci/Mmol, New England Nuclear, Boston, Mass.).

RADIOAUTOGRAPHIC TECHNIQUE: Radioautography was carried out on animals perfused with paraformaldehyde at 2, 5, 10, 20, 30, and 90 min and 4 and 30 h and the tissues were prepared as follows. For light microscope radioautography 0.5-μm Epon sections were mounted on glass slides, stained with iron hematoxylin, coated with NTB2 emulsion (33), and exposed at 4°C for 3 days to 3 wk. The radioautographs were developed in D170 for 6 min at 18°C and fixed for 3 min in 24% sodium thiosulfate.

For electron microscopy, sections (with pale gold interference color) were mounted with a wire loop on glass microscope slides previously coated with 0.8% celloidin. Using the semiautomatic device developed by Kopriwa (32), the slides were dipped into Ilford L4 emulsion (Ilford Ltd., Ilford, Essex, England) diluted 1:3 with distilled water. The radioautographs were developed either in D19b, a well-standardized procedure yielding thread-like silver grains and used for quantitation, or in a solution-physical developer which provided small compact silver grains (Figs. 33–40) as described by Kopriwa (31). Staining of thin sections was carried out for 20-30 min with lead citrate.

QUANTITATIVE RADIOAUTOGRAPHY: Light microscope quantitation was carried out on sets of semithin sections that were coated at the same time and developed after 3 days exposure. In the case of the 2-min interval, however, the exposure time was 21 days and a correction made. Silver grains were counted over a selected area in a Zeiss micrometer inserted into the × 10 ocular of a microscope fitted with an × 100 objective. Each square of the micrometer included an area of 100 μm^2. The section was adjusted so that squares were positioned over cells, predentin, or dentin and the silver grains were enumerated in these three areas. In predentin the grains over odontoblast processes were recorded separately from those over the predentin matrix and added to those counted over the cells. The results were expressed as number of silver grains over cells (including odontoblast processes), predentin, and dentin (Table I, left). The percentage of silver grains over cells and predentin, excluding dentin, was then calculated (Table I, right).

Using comparable areas on semithin sections,

TABLE I

Counts of Silver Grains in the Light Microscope over Odontoblasts, Adjacent Predentin, and Dentin in Semithin Sections at Various Time Intervals after [^{3}H]Proline Injection

	Number of silver grains				Percent silver grains (excluding dentin)	
Time interval	Total	Cell (+ odontoblast process)	Predentin	Dentin	Cell (+ odontoblast process)	Predentin
2 min	56	55	0	1	100	0
5 min	58	56	2	0	96.6	3.4
10 min	86	84	1	1	98.8	1.2
20 min	267	263	3	1	98.9	1.1
30 min	424	329	94	1	77.8	22.2
90 min	420	102	310	8	24.8	75.2
4 h	455	65	378	12	14.7	85.3
30 h	415	37	85	293	—	—

an index of the relative volumes occupied by cells (including odontoblast processes) and predentin was determined by counting the number of hits of micrometer square intersections and expressing the results as a percentage of the number of point hits (Table II).

On the basis of light microscope radioautographs it became apparent that the supranuclear, Golgi, and apical regions of the odontoblasts (including the processes) and the adjacent predentin were the areas to be considered for electron microscope quantitation. The infranuclear region contained little radoactivity and was not included for grain counting in electron micrographs. Counts were carried out on 8- by 10-inch photographs at a magnification of × 30,000 prepared from radioautographs developed in D19b. Silver grains were recorded over the following structures: (*a*) rough endoplasmic reticulum, (*b*) Golgi apparatus, including flattened and distended portions of saccules, (*c*) secretory granules, including those in the Golgi region, apical cytoplasm, and odontoblast process, (*d*) predentin, and (*e*) other structures. The grains were examined at each time interval by the method of Nadler (81). In the case where a single organelle was within a circle (an exclusive grain) one point was assigned to the organelle, whereas, if a silver grain overlaid two structures, e.g. Golgi saccule and secretory granule, it was considered a shared grain and the structures were assigned half a point each (Table III). An index of the relative volume occupied by the components of the odontoblasts in photographs of whole cells was determined by the "point hit" method of Chalkley (9, 40) and expressed as a percentage of the number of point hits (Table IV). The relative volumes occupied by odontoblast components and predentin was assessed by recording

TABLE II

Percent Hits in the Light Microscope on Odontoblasts and Predentin in Semithin Sections

	Percent hits*
Cell + odontoblast process	67.1
Predentin	32.9

* Determined from a total of 3,910 hits.

TABLE IV

*Percent Hits on Odontoblast Components (Including Processes) in Electron Micrographs**

Component	Percent hits
rER	39.8
Golgi apparatus	15.9
Secretory granules	2.0
Mitochondria	4.1
Odontoblast process‡	16.1
Others	22.0

* Determined from a total of 2,256 hits.
‡ Excluding secretory granules.

TABLE V

*Percent Corrected Hits on Odontoblast Components and Predentin**

Component	Percent hits
rER	26.7
Golgi apparatus	10.7
Secretory granules	1.3
Mitochondria	2.8
Odontoblast process	10.8
Others	14.7
Predentin	33.0

* Determined by expressing the percent hits from Table IV as a fraction of percent hits over cell and odontoblast process, i.e. 67% (assuming from Table II that the percent hits over predentin is 33%).

TABLE III

Counts of Silver Grains over Odontoblasts and Associated Predentin in Electron Micrographs of Thin Sections at Various Time Intervals after [^{3}H]Proline Injection

Time interval	Number of silver grains	Percent silver grains at each time interval				
		rER	Golgi apparatus	Secretory granules	Predentin	Others
2 min	79	94	2	—	—	4
10 min	637	81	13	—	—	6
20 min	406	40	50	6	—	4
30 min	637	23	34	15	18	10
90 min	685	3	1	5	88	3
4 h	963	1	—	1	94	4

the per cent point hits over odontoblast components as a fraction of 67% (which is the volume occupied by cells relative to that occupied by predentin, as shown in Table II) and expressing the results as percentages of corrected point hits (Table V). Finally, an index of the relative concentration of grains per structure at each time interval was obtained by dividing the percent grain counts by the percent point hits on the structure. The results for rough endoplasmic reticulum, Golgi apparatus, secretory granules, and predentin are recorded in Fig. 41.

Blood Plasma Clearance of Radioactivity with Time after Intravenous Injection of [^{3}H]Proline

Blood plasma clearance was determined by administering 50 μCi of L-[2,3-^{3}H]proline (45.7 Ci/Mmol, New England Nuclear) in a volume of 0.2 ml into the jugular vein of ether-anaesthetized 40-g Sherman male albino rats. Three animals per time

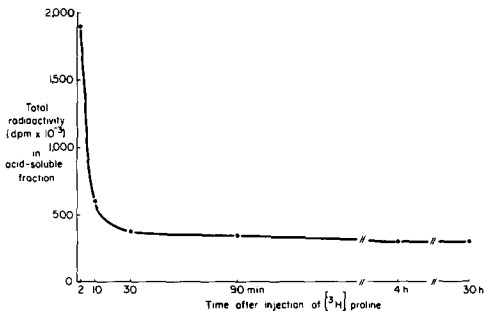

FIGURE 1 Radioactivity present in the acid-soluble fraction of blood plasma (attributable to free [^{3}H]-proline) at various time intervals after intravenous injections of [^{3}H]proline into 40-g rats. The values are the averages of samples taken from three animals per time interval. The sharp drop during the first 10 min after injection indicates that a pulse of high radioactivity is achieved by the injection. Between 30 min and 30 h, a plateau is reached, indicating the persistence of some radioactivity in the acid-soluble fraction of the plasma throughout the experimental period.

FIGURES 2–4 Light micrographs and diagrammatic representation of rat incisor odontoblasts.

FIGURE 2 Light micrograph of a transverse section through the rat maxillary incisor within the proximal third of the growing end. The section was stained with toluidine blue. The secretory ameloblasts (*A*) and the intensely stained enamel (*E*) are located on the labial surface of the tooth, seen at the top of the figure. Below, the pulp occupies a large space at this level of section. Along the periphery of the pulp (*P*) is a dark staining layer of cells composed of the odontoblasts (*Od*). In the present study attention was directed to the odontoblasts on the labial surface. Adjacent to the odontoblasts is a light staining layer of predentin, beyond which is the slightly darker staining dentin (*D*). × 45.

FIGURE 3 Odontoblasts (*Od*), predentin (*Pd*), and dentin (*D*) from the growing end of the rat incisor as they appear in semithin sections stained with toluidine blue. The tall, well-polarized odontoblasts are arranged parallel to one another. The nuclei are found at the base. A centrally located, circumscribed, clear area corresponds to the Golgi region (*G*). Above and below this region are darker staining areas corresponding to the supranuclear rER (*SrER*) and apical rER (*ArER*). The latter lies beneath the terminal web region (*Tw*). Extending into the predentin from each cell is the light staining odontoblast process (*Op*). Although these processes are continuous through predentin and dentin, they are frequently viewed in tangential section. Predentin extends from between the base of the processes to a sharply defined predentin-dentin junction (black arrow). The dentin is located beyond, and stains darker than predentin. × 1,000.

FIGURE 4 Diagrammatic representation of the odontoblast from the region under investigation. This cell is slender and its nucleus basally located. The well-developed Golgi region generally occupies a large circumscribed area around the cell center and contains profiles of Golgi saccules and granules as well as multivesicular bodies. Above and below are elaborate arrays of flattened cisternae of rough endoplasmic reticulum (*rER*) oriented along the long axis of the cell and referred to here as the supranuclear rER and apical rER. Mitochondria are frequently found in these regions as well as around the Golgi apparatus. Apical junctions are present between adjacent cells and give rise to an incomplete terminal web. Beyond the terminal web extends the odontoblast process, consisting of cytoplasmic ground substance from which the rER is excluded. The process is surrounded by, and embedded in the predentin and dentin matrix. Predentin matrix is excluded from the intercellular spaces below the apical junctions and is composed of collagen fibrils and interfibrillar material. Collagen fibrils increase progressively in size and abundance from the proximal predentin to the dentin. Beyond the predentin-dentin junction, collagen fibrils possess a particulate material on their surface. The area immediately beyond the junction is the site of dentin mineralization.

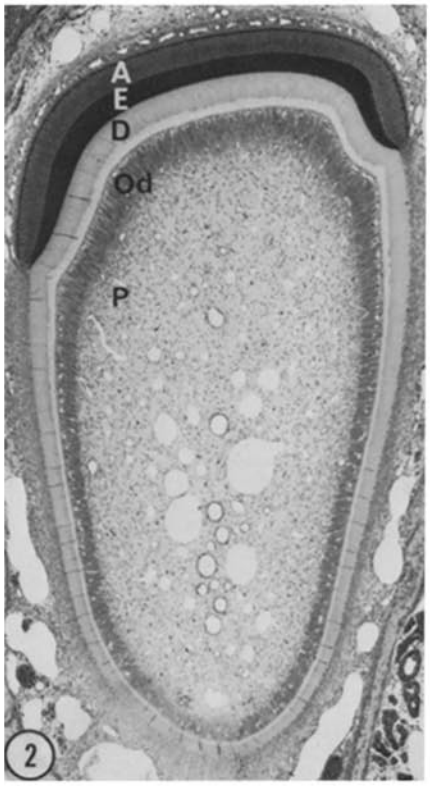
A
E
D
Od
P
2

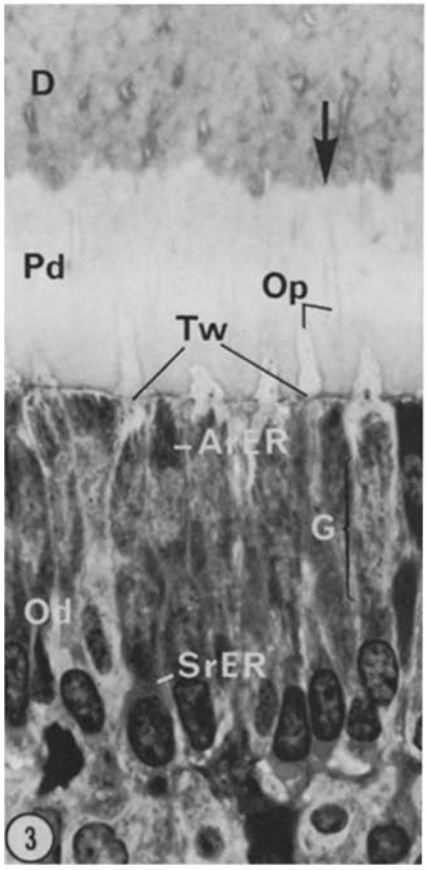
D
Pd
Op
Tw
A ER
G
Od
SrER
3

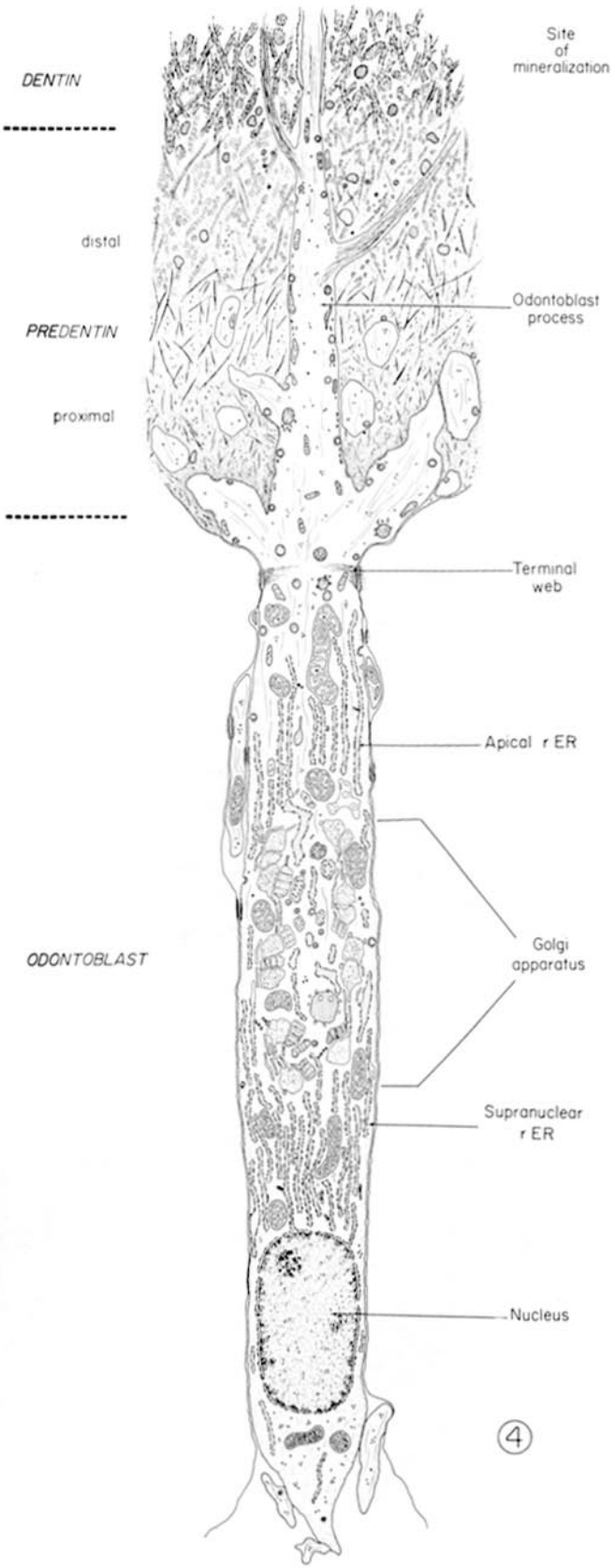
DENTIN
distal
PREDENTIN
proximal
ODONTOBLAST
Site of mineralization
Odontoblast process
Terminal web
Apical r ER
Golgi apparatus
Supranuclear r ER
Nucleus
4

interval were used for separate determinations. The animals were exsanguinated through the abdominal aorta with a 20-gauge needle attached to a heparinized syringe at times ranging from 2 min to 30 h. The whole blood was centrifuged and the plasma proteins and glycoproteins precipitated in a mixture of 12% trichloracetic acid and 1.7% phosphotungstic acid. The precipitates were washed in the same mixture diluted with an equal amount of water. 50-μl samples of the collected supernatant fractions were added to diotol and the radioactivity measured in a Packard Tri-Carb, model 3003, liquid scintillation spectrometer (Packard Instrument Co., Downers Grove, Ill.). The acid-soluble radioactivity in the supernatant samples was considered to be an index of the amount of free [^{3}H]proline, particularly at early time intervals (Fig. 1).

RESULTS

Morphological Observations

Light Microscopy

The odontoblasts examined in this investigation are located at the labial surface of the maxillary incisor tooth near its growing end (top of Fig. 2). They make up a layer of narrow polarized columnar cells approximately 50 μm tall (Fig. 3). The Golgi region appears as a clear area centrally located in the cell body. Beyond the terminal web is a light-staining cytoplasmic extension, the "odontoblast process," which projects into, and is enveloped by, the predentin and dentin matrix. The base of the process appears pale and contains granules at the limit of visibility.

The light-staining predentin matrix, which is unmineralized (64, 71), extends from the region between the base of the processes for a thickness of about 30 μm up to a sharply defined predentin-dentin junction (Fig. 3). The dentin matrix, which is mineralized (64, 71), takes up the stain readily and appears dark. Predentin and dentin contain profiles of odontoblast processes in various planes of section.

Electron Microscopy

Since the arrangement of the organelles in odontoblasts has been described previously (19, 43, 53, 54, 65), only those features which will be useful for the interpretation of the biosynthesis of collagen will be described.

STRUCTURE OF THE ODONTOBLAST: The structure of the odontoblast is summarized diagrammatically in Fig. 4. The nucleus separates an infranuclear region, containing few organelles, from a supranuclear region in which abundant profiles of cisternae of the rough endoplasmic reticulum may be discerned (Fig. 5). The cisternae consist of long, flattened, interconnected profiles stacked adjacent to each other (Fig. 5, right). They are usually absent from the region immediately below the terminal web and from the odontoblast process (Figs. 5, 6, 18). A large Golgi apparatus occupies the central region of the cell body, where some elements of the rough endoplasmic reticulum may penetrate (Figs. 7, 10).

Other cytoplasmic components include mito-

FIGURES 5 and 6 Portions of odontoblasts and process sectioned longitudinally.

FIGURE 5 Portions of odontoblasts sectioned longitudinally. The cell in the left part of the picture has been sectioned close to its central axis. Abundant profiles of rER oriented along the long axis of the cell may be seen in the supranuclear (*SrER*) and apical regions (*ArER*). However, the uppermost apical region, located below the level of the junctions (circles) and associated terminal web (*Tw*), is usually lacking in rER. The rER is also excluded from the odontoblast process (*Op*), which is considered to begin at the terminal web. Mitochondria (*M*) are present throughout the cell body but are generally absent from the process. Between the supranuclear and apical rER, the extensive Golgi apparatus occupies a circumscribed area in the cell center. Nucleus (*N*), predentin (*Pd*), gap junction (arrow). × 7,500.

FIGURE 6 Profile of a portion of an odontoblast process cut along its length, with the predentin (*Pd*) on either side. Secretory granules (*Sg*) may be seen deep within the process and adjacent to the plasma membrane. A coated vesicle (*Cv*), dense bodies (*Db*), and smooth membrane elements (*Sm*) are also found. The ground substance contains filaments and microtubules (*Mt*). Since the section was stained with lead only, collagen fibrils generally appear as white lucent profiles in the extracellular matrix (*75*). The membrane-limited profiles in the matrix (arrowheads) probably correspond to branches from the main trunk of the odontoblast process in various planes of section. At Ag an aggregate comparable to that seen in Fig. 18, inset, may be seen. × 15,000.

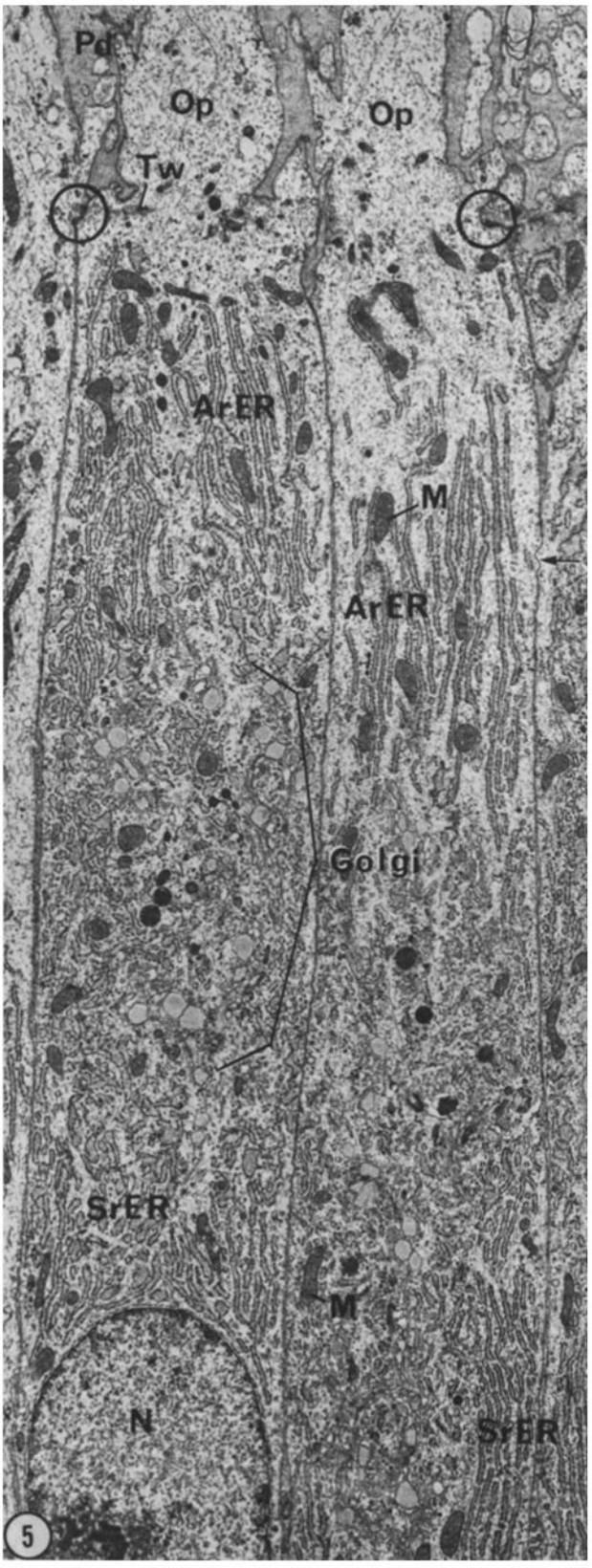
Pd
Op
Op
Tw
ArER
M
ArER
Golgi
SrER
M
N
SrER
5

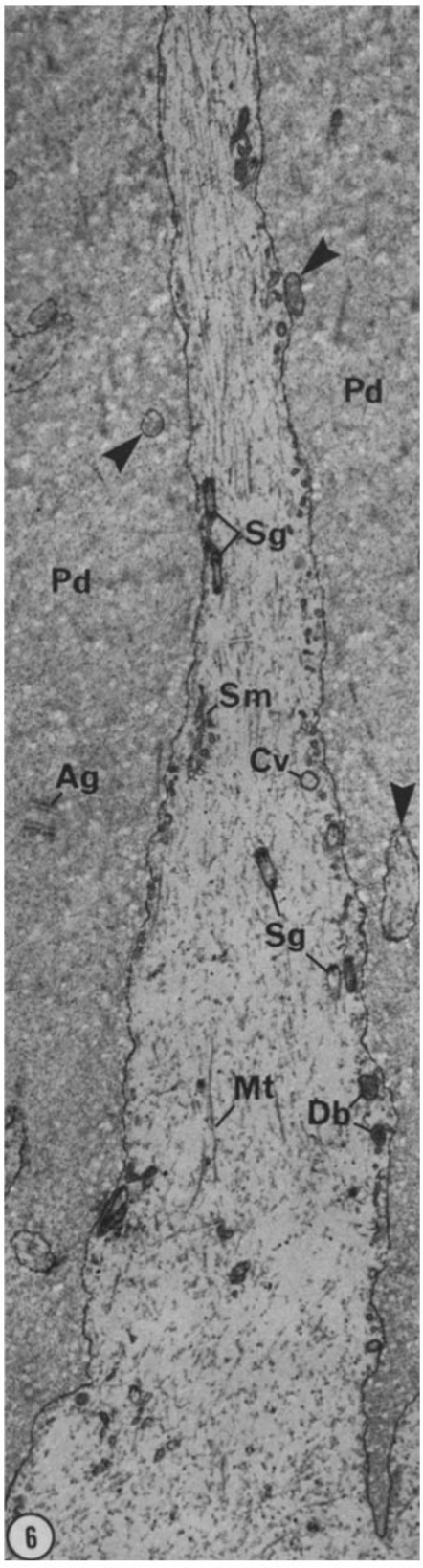
Pd
Sg
Pd
Sm
Cv
Ag
Sg
Mt
Db
6

chondria, dense and multivesicular bodies, as well as free ribosomes, glycogen particles, filaments, and microtubules. There are also membrane-bound elongated profiles containing electron-dense material, particularly in the apical cytoplasm (Fig. 18, Sg). For reasons that will become evident below, these structures are referred to as secretory granules.

GOLGI APPARATUS: The Golgi apparatus, depicted diagrammatically in Fig. 42, consists of interconnected stacks of flattened fenestrated saccules, usually four per stack (Figs. 7, 8). Sac-like distensions which may occur along the length of the saccules (Figs. 7, 10) or at their periphery (Figs. 8, 9) are among the most conspicuous components.

Along the side of a Golgi stack identified as the proximal (forming) face, lie flattened cisternae of the rough endoplasmic reticulum, some of which have lost their ribosomes and may be considered to be transitional elements (Figs. 7, 9). Fuzz-coated vesicles with a diameter of 50 nm are also frequent components of this region (Figs. 8, 10) and contain a moderately electron-dense material. They are considered to be intermediate or transitional vesicles. Buds resembling these vesicles are connected to distended or flattened portions of saccules (Figs. 10, 42).

The distended portions of the first (Fig. 7, DS1) and second (Fig. 9, DS2) saccules usually have an irregular circular profile and are considered to be spheroidal in their three-dimensional configuration. They will be referred to as "spherical portions." They contain a mat of entangled filamen-

FIGURES 7–10 Portions of the Golgi apparatus from odontoblasts.

FIGURE 7 At top left, profiles of rough endoplasmic reticulum cisternae (*rER*) and a microtubule (*Mt*) may be observed. Below, double arrows indicate smooth membraned elements. One of these elements (*Te*) is continuous with a portion displaying ribosomes and is considered to be a transitional element. A stack of Golgi saccules (*S1–S4*) extends beyond the photographic field; the saccules show interruptions indicating the presence of fenestrations. Large spherical profiles such as the one labeled *DS1* in the bottom of the photomicrograph represent the distended portion of the first saccule of the stack (*S1*) and contain finely entangled threads. At the top of the photomicrograph, a cylindrical profile labeled *DS3* contains faintly stained threads parallel to one another; densities appear on the threads at a repeating interval. Other elongated profiles (*PSg*) are seen, which apparently lie free in the cytoplasm. They contain parallel threads and, in addition, regularly arranged, electron-dense, spheroidal particles. The surface of these profiles (*PSg*) displays bristle-coated areas and buds (arrow); these profiles are considered to be prosecretory granules. The same side of the Golgi apparatus (distal face) exhibits bristle-coated vesicles (*Cv*). × 60,000.

FIGURE 8 At the left side of the figure, smooth membrane elements (double arrows) and an intermediate vesicle (*v*) may be seen. At top of figure, a distended portion of a saccule (*DS3*) shows parallel threads and appears to be confluent with a flat portion of a Golgi saccule (*S3*) which is part of a stack of flattened saccules (*S1–S4*). The limiting membrane of some elongated profiles (*PSg*) sectioned tangentially possess bristle-coated areas (black arrowhead). Other profiles contain homogeneously staining material (*Sg*). Both types of profiles are free in the cytoplasm, contain electron-dense particles, and are referred to as prosecretory and secretory granules respectively. Bristle-coated vesicles (*Cv*) are abundant in this region. × 60,000.

FIGURE 9 From left to right, the figure depicts a transitional element (*Te*), several smooth membraned profiles (double arrows), a microtubule (*Mt*), and a stack of four Golgi saccules (*S1–4*). A distended portion (*DS2*) of saccule 2 is also present and contains fine entangled threads. A profile of a prosecretory granule in cross section is also in the field (*PSg*). × 60,000.

FIGURE 10 In this photomicrograph a distended portion of saccule (*DS1*) is contiguous with tubular elements which appear to interconnect with flattened portions of saccules. At center left, a distended portion (*DS4*) shows parallel threads grouped into several small bundles with a cross periodicity. The arrow at upper left identifies a fuzz-coated bleb confluent with the flattened portion of a saccule, adjacent to the site where it opens into DS4, while the arrow at lower right identifies a fuzz-coated bleb contiguous with DS1. A fuzz-coated vesicle (*v*) lies free in the cytoplasm. Also seen is a portion of the rough endoplasmic reticulum (*rER*). × 50,000.

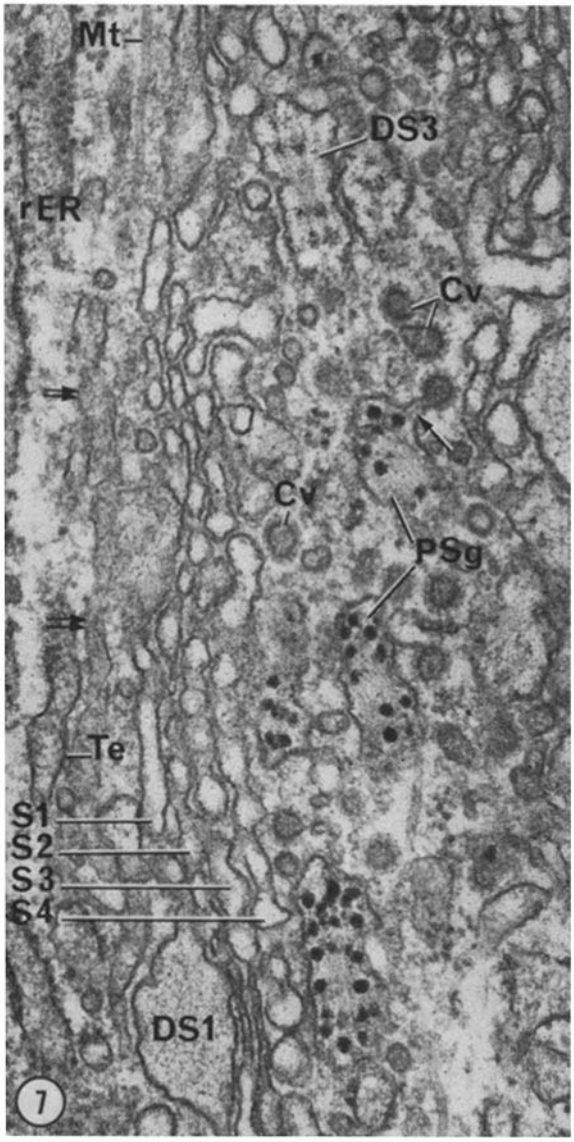
Mt
DS3
rER
Cv
Cv
PSg
Te
S1
S2
S3
S4
DS1
7

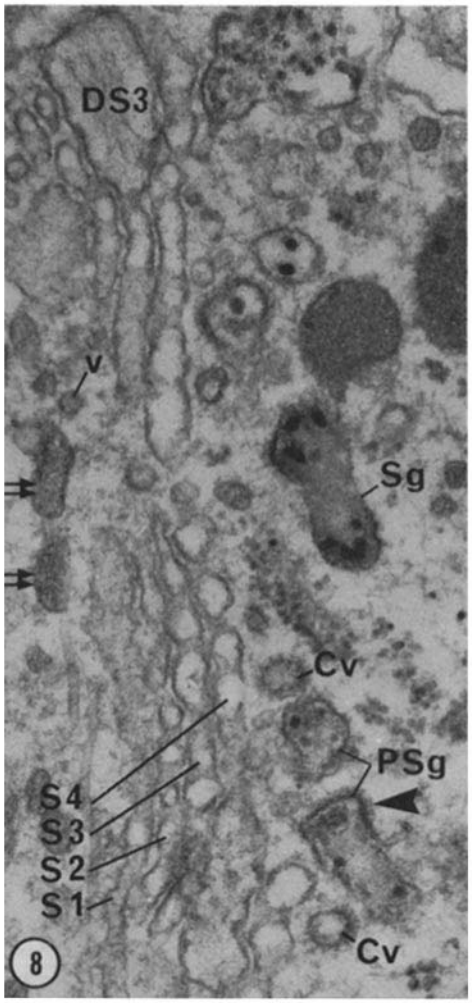
DS3
v
Sg
Cv
PSg
S4
S3
S2
S1
Cv
8

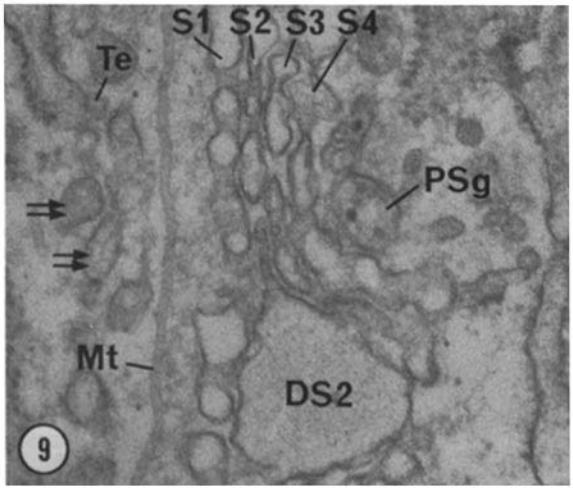
S1 S2 S3 S4
Te
PSg
Mt
DS2
9

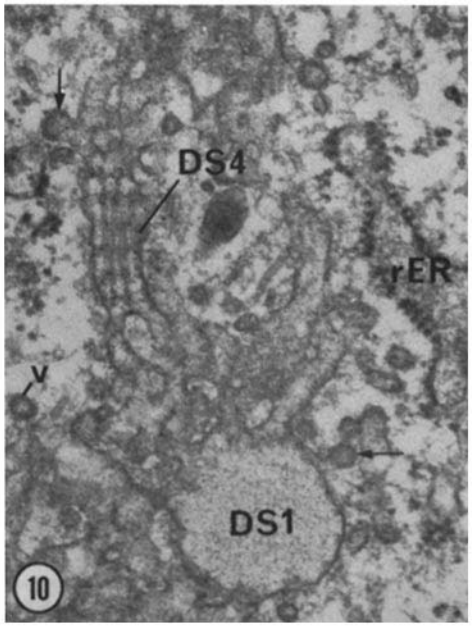
DS4
rER
v
DS1
10

tous threads measuring approximately 2 nm in thickness (Fig. 11).

Towards the distal (secretory or mature) face of the Golgi saccules, the profiles of the distended portions of the third (Fig. 8, DS3) and fourth (Fig. 10, DS4) saccules are usually rectangular and will be referred to as "cylindrical portions." They contain distinct filamentous threads oriented in parallel along the long axis of the profile. The threads (Fig. 12) may be loosely associated into a bundle (Fig. 13) referred to as an "aggregate." In some profiles, the threads are more closely associated (Figs. 14, 15); five major densities are evident along the aggregates with a periodic spacing of approximately 70 nm. The middle density usually stains more weakly than the others (Fig. 14), and a sixth density (Fig. 15) may also be present. The aggregates measure 280–350 nm in length. When cylindrical portions of saccules are viewed in cross section, the aggregates may be seen to be composed of small bundles of threads which are also evident in sections stained with lead citrate alone (75) and in sections stained with silver methenamine (Fig. 24).

Elongated profiles which do not appear to be attached to saccules are regular components of the Golgi region. They have an approximate length of 400 nm and a width of 150 nm. In some of these profiles, the aggregated threads are distinguishable. The limiting membrane is irregular and may show bristle-coated patches (Fig. 8) and small stalks connected to bristle-coated blebs, which measure about 100 nm in diameter (Fig. 7). Free bristle-coated vesicles lie nearby in the cytoplasm. These profiles also contain intensely opaque spheroidal particles which measure 30 nm in diameter (Fig. 7, Psg) and are often aligned in register with the electron opacities of the aggregates (Fig. 16). The elongated profiles displaying these various features are referred to as "prosecretory granules."

Other elongated profiles of the Golgi region possess a regular limiting membrane and are slightly smaller in dimensions than prosecretory granules. The content of these profiles stains homogeneously with the routine uranium-lead stain, and aggregated threads are not readily discernible (Fig. 8); however, 30-nm electron-opaque particles are present. These elongated profiles are referred to as "secretory granules." Their size, shape, and content is comparable to those of the secretory granules noted in the apical cytoplasm (Figs. 17, 18) as well as those present in the odontoblast process described below.

ODONTOBLAST PROCESS: The odontoblast possesses a long process extending from the terminal web region into the predentin and dentin matrices (Figs. 4, 18). This process consists of a main trunk continuous with the cell body and of smaller branches which project from the basal portion into the substance of the predentin. Both trunk and branches taper towards their tips.

Mitochondria are rarely, and cisternae of the endoplasmic reticulum and Golgi stacks are never, found in the process. However, secretory granules,

---

FIGURES 11–17 These figures show presumptive changes in the shape of the distended Golgi saccules and in the organization of their contents during the events leading to the formation of secretory granules (Fig. 17). The material was fixed in glutaraldehyde. × 100,000.

At an early stage (Fig. 11) corresponding to the spherical portions described as DS1 in Figs. 7 and 10, a mat of entangled fine filamentous threads is present. The threads may be in close association with the limiting membrane of the saccule (arrow). At a subsequent stage (Fig. 12) the profile is elongated and the threads are oriented along its long axis. In Fig. 13, the saccule is cylindrical and contains filamentous threads aligned in parallel with a faint electron density at repeating intervals (arrows). This electron-dense periodicity is more pronounced in saccules where the threads become more condensed (Fig. 14). The limiting membrane of such saccules may possess blebs on its surface (black arrowhead in Fig. 14). Subsequent stages apparently involve further condensation of the filamentous content and accentuation of the periodic densities (Fig. 15). Most frequently five densities appear along the condensed aggregates and, after uranyl and lead staining, the central one is the least prominent (Fig. 14). A sixth may also be present (Fig. 15). As already described in Fig. 7, electron-dense, 30-nm particles become aligned within the content of elongated granules (Fig. 16). They are arranged with a periodic spacing of about 70 nm, like the periodically spaced densities associated with the filamentous threads. A mature secretory granule may be seen in Fig. 17. Electron-dense, 30-nm particles are in evidence, particularly along the periphery of the limiting membrane.

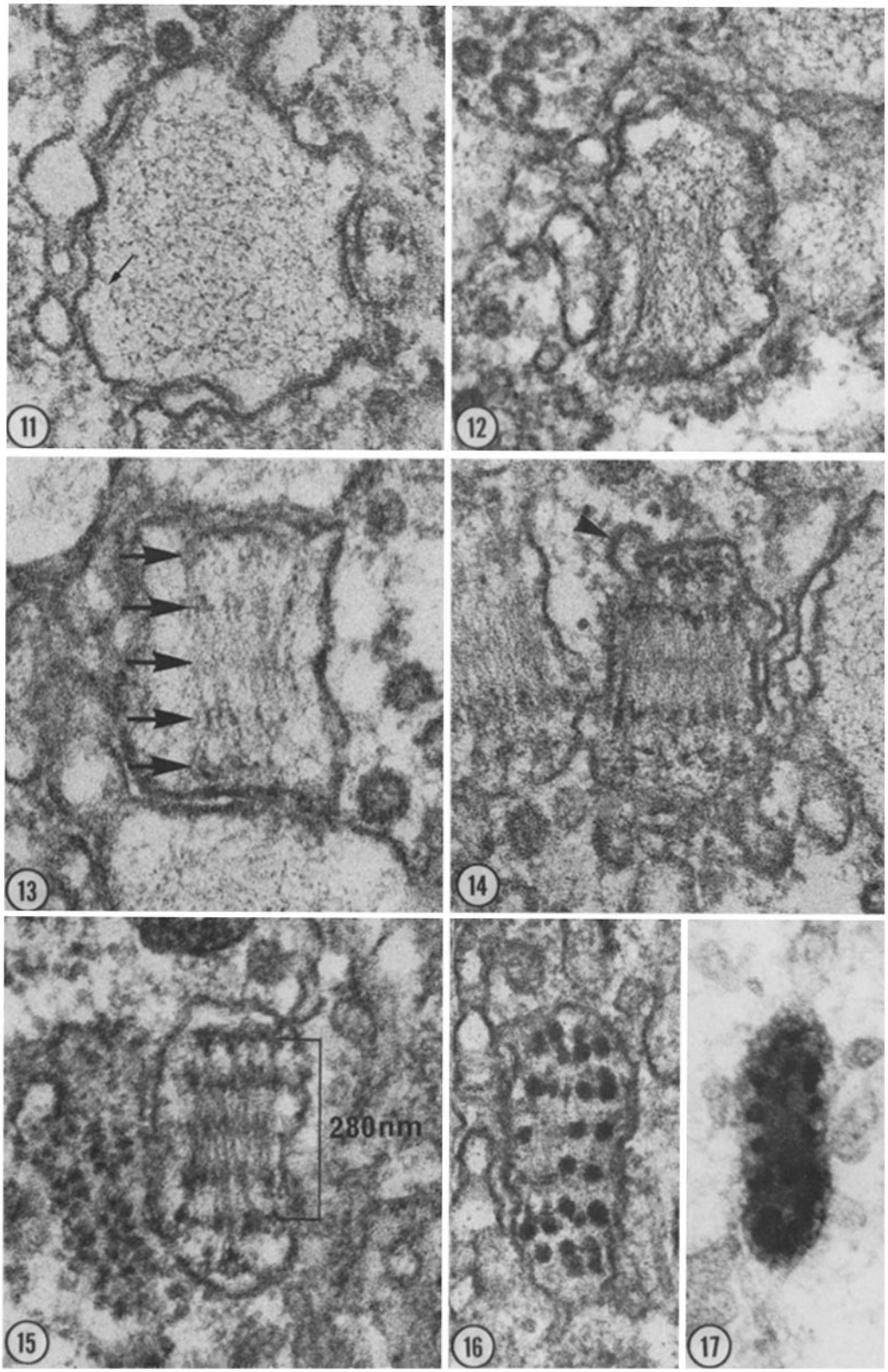
11
12
13
14
280nm
15
16
17

dense bodies, large bristle-coated vesicles, and smooth membrane elements are present (Figs. 6, 18, 19). Secretory granules may be found adjacent to the plasmalemma or deep within the process (Figs. 6, 19). They contain a homogeneous material of moderate opacity comparable to the collagen fibrils in the adjacent predentin as well as intensely electron-opaque particles (Fig. 19).

Examination of the cell surface along the odontoblast process reveals the presence of invaginations of the plasmalemma, such as the one depicted in Fig. 20. In profile the content appears floccular and somewhat filamentous and is similar to the material in the adjacent predentin matrix although more densely packed. Invaginations of the plasmalemma such as the one depicted in Fig. 21 were also noted frequently, particularly at the base of the odontoblast process. These concavities routinely possess moderately electron-dense structures adjacent to the cell surface. These can be distinguished at low magnification (Fig. 18, arrowhead). At high magnification, they appear aligned in a regular array a short distance from the cell surface (Fig. 21). The central part of the invagination appears light and contains a loosely filamentous material similar to the more condensed predentin matrix material. Although Figs. 20 and 21 were obtained from undemineralized tissues fixed in a solution of formaldehyde-glutaraldehyde in cacodylate buffer, a similar pattern was observed after other fixations. The sequence depicted in Figs. 19–21 has been included to show what appears to be the mechanism whereby the secretory granules release their content to the cell surface by exocytosis.

PREDENTIN MATRIX: The predentin consists of proximal and distal regions (Fig. 4) showing a gradual transition from one to the other. Both contain collagen fibrils. In the proximal predentin these are embedded in an abundant, finely

---

FIGURES 18–21 Portions of odontoblast processes (Fig. 18) and presumed steps in the release of content of secretory granules (Figs. 19–21).

FIGURE 18 Apical regions of odontoblasts showing profiles of odontoblast processes (*Op*) and their minor branches in various planes of section. The terminal web which is well defined in the cell at left (*Tw*) is taken as the boundary between cytoplasm and odontoblast process. Secretory granules (*Sg*) and dense bodies (*Db*) are regular components of the process; however, the rough endoplasmic reticulum is excluded. At low power, the proximal predentin is finely granular and shows randomly arranged collagen fibrils. These become abundant in distal predentin (top of figure). On the external surface of the plasmalemma, particularly in the proximal portions of the odontoblast process where secretory granules are frequently encountered, electron-dense accumulations may be distinguished (arrowhead). Other elements occasionally detected in predentin (inset at upper left) are not believed to be typical collagen fibrils but rather aggregates of tropocollagen or procollagen molecules. These aggregates measure about 300 nm in length, are of variable width, and appear to be composed of thin, parallel threads. They possess a symmetrical cross-banding pattern. × 14,400. *Inset*, × 90,000.

FIGURE 19 Secretory granule (*Sg*) in a portion of odontoblast process (lower right) with nearby predentin (upper left) routinely stained with uranyl acetate and lead citrate. The secretory granule shows a moderately electron-dense homogeneous content that resembles in staining properties the collagen fibrils (*Col*) distinguishable in the adjacent predentin matrix. Electron-dense particles are also present in the granule. The granule lies adjacent to the plasmalemma. Cytoplasmic filaments are at lower right. ×60,000.

FIGURE 20 Secretory granule in the proximal portion of the odontoblast process. The limiting membrane of the granule may be seen confluent with the plasma membrane of the process (arrow). There is evidence of the presence of filament bundles (arrowhead) of the length of those observed in cylindrical Golgi saccules. Presumably, extrusion of the granule content into the predentin matrix (upper left) will ensue. A collagen fibril (*Col*) and threads of various sizes may be seen in the predentin. × 60,000.

FIGURE 21 Secretory granule discharge in a region of the odontoblast process similar to that seen in Fig. 18 (arrowhead). The granule membrane is continuous with and part of the plasmalemma in the region between the arrows. The regular pattern of electron-dense accumulations on the external surface of the plasmalemma may be seen to advantage. A clear area within which delicate threads are visible in various planes of section may be identified in the central region. × 60,000.

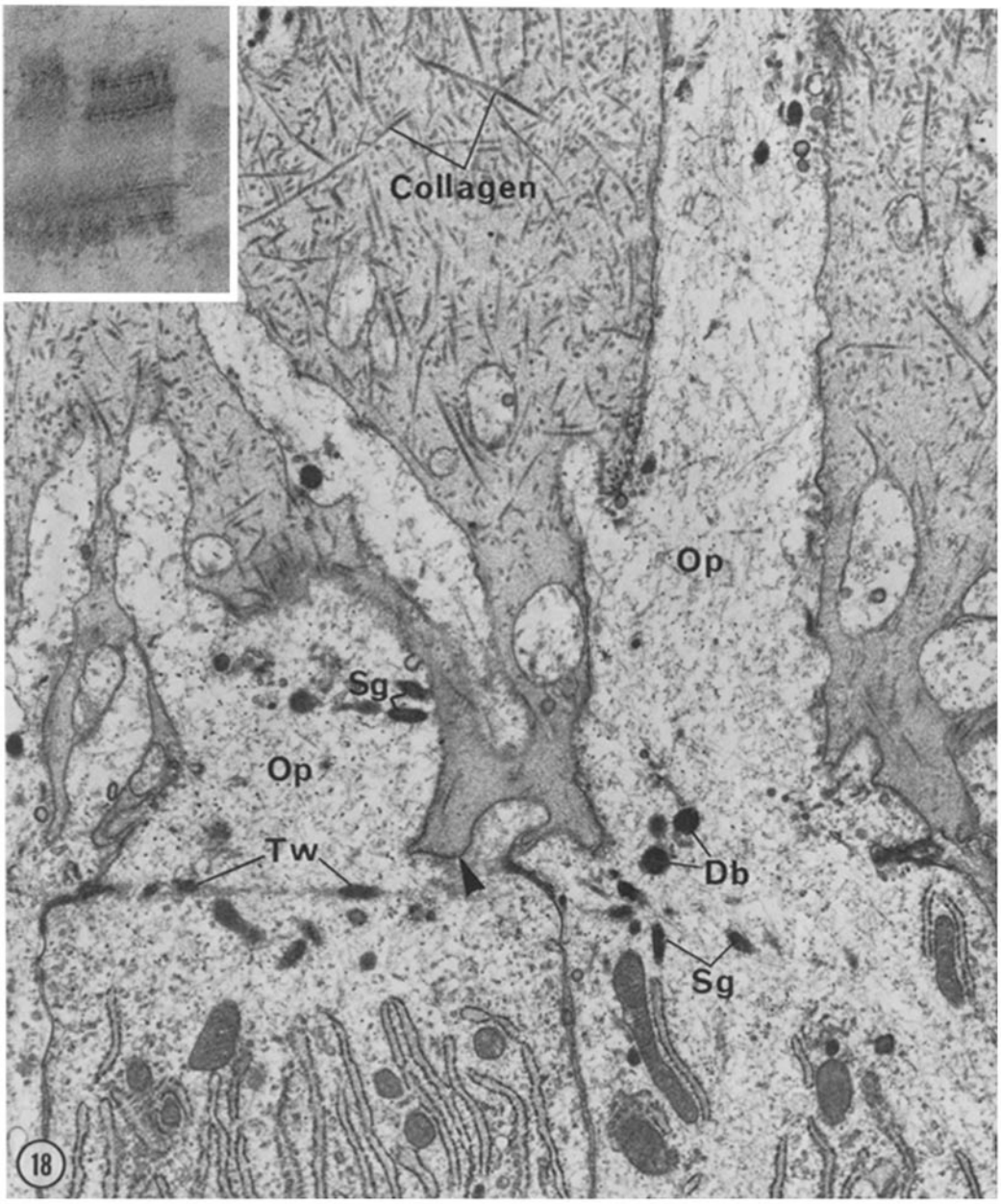
Collagen
Op
Sg
Op
Tw
Db
Sg
18

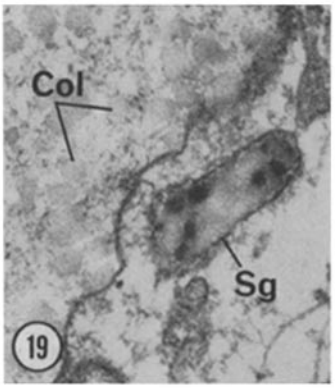
Col
Sg
19

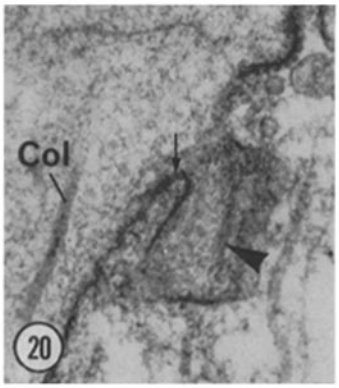
Col
20


21

stippled material (Fig. 18), which is also present in lesser amounts within the distal predentin. At high magnification this material appears to be composed of very small filaments. In the proximal predentin, the collagen fibrils are regular in diameter (20–30 nm) and may be observed deep within predentin as well as within scalloped depressions of the plasma membrane (Fig. 19). As distal predentin is approached, the proportion of collagen fibrils to interfibrillar material increases as does the average diameter of the collagen fibrils.

Other elements distinguishable from collagen fibrils were occasionally encountered in the predentin (Fig. 18, inset). These elements have a length of the order of 300 nm and vary in their width. Cross bands are evident on either side of a moderately staining central region, and fine parallel threads which appear to comprise these elements run perpendicular to the cross bands. These structures bear certain features similar to those of the aggregates of parallel threads described in the distended portions of Golgi saccules. For example, the symmetrical banding pattern of the predentin aggregates is comparable to the symmetry of the major density pattern of the Golgi aggregates (Fig. 14). It should be pointed out that the aggregates in predentin were not a routine finding in the thin sections examined. When present, however, they often appeared in groups within the proximal predentin, adjacent to the plasmalemma as well as deep in the matrix.

Histochemical Observations

With the realization that collagen is a glycoprotein containing galactose and glucose residues (5, 61), we decided to treat odontoblasts and the adjacent matrix with the phosphotungstic acid stain at low pH for the detection of glycoprotein (50, 52). In addition, since collagen fibrils are known to stain with silver methenamine (51), this reagent was also applied to the material under study.

STAINING WITH PHOSPHOTUNGSTIC ACID AT LOW PH: Within the odontoblasts, staining predominated in the Golgi region (Fig. 22). In the spherical portions (DS1, DS2) of Golgi saccules, the periphery was moderately stained. In the cylindrical portions (DS3 and DS4), the staining was pronounced and localized to the aggregates of parallel threads. The structures referred to as prosecretory and secretory granules were also intensely stained. In some of these, five or six cross bands more intensely stained than the surrounding content could be distinguished (Fig. 22, inset). These cross bands were present in the same location as the 30-nm particles depicted in Fig. 16.

Within the odontoblast process (Fig. 23) as well as within the apical cytoplasm, the secretory granules stained intensely, and a cross band pattern was distinguishable in a few of them. Dense and multivesicular bodies also stained.

In the predentin and dentin matrix, collagen fibrils took up the stain (Fig. 23).

STAINING WITH SILVER METHENAMINE: In odontoblasts, an electron-opaque precipitate of silver was observed in the Golgi region, where it was localized to certain saccules containing groups of elements aligned in parallel (Fig. 24, DS4). These correspond to the aggregates of parallel

---

FIGURES 22 and 23 Electron micrographs of portions of odontoblasts stained for glycoprotein. The decalcified teeth were embedded in glycol methacrylate and the sections treated with *phosphotungstic acid at low pH*.

FIGURE 22 In the Golgi region, a rim of stain is visible in the spherical portions of Golgi saccules (*DS1*), whereas the central part remains unstained. At later stages the bundles of parallel threads in cylindrical portions take up the stain (*DS4*), and secretory granules (*Sg*) are intensely stained. The inset represents a stained secretory granule in which the reaction predominates in regions corresponding to the sites where electron densities (Fig. 15) and small particles (Figs. 16, 17) become associated with the thread-like content (arrows). An additional site that takes up the stain is the cell coat at the free surfaces of adjacent cells (*CC*). × 21,600. *Inset*, × 80,000.

FIGURE 23 From top to bottom in center is a portion of the odontoblast process sectioned longitudinally. The secretory granules (*Sg*) seen in longitudinal and cross section are intensely stained. Multivesicular bodies and dense bodies (*Db*) also stain. In the predentin matrix, collagen fibrils display intense staining, whereas the interfibrillar substance does not. × 21,600.

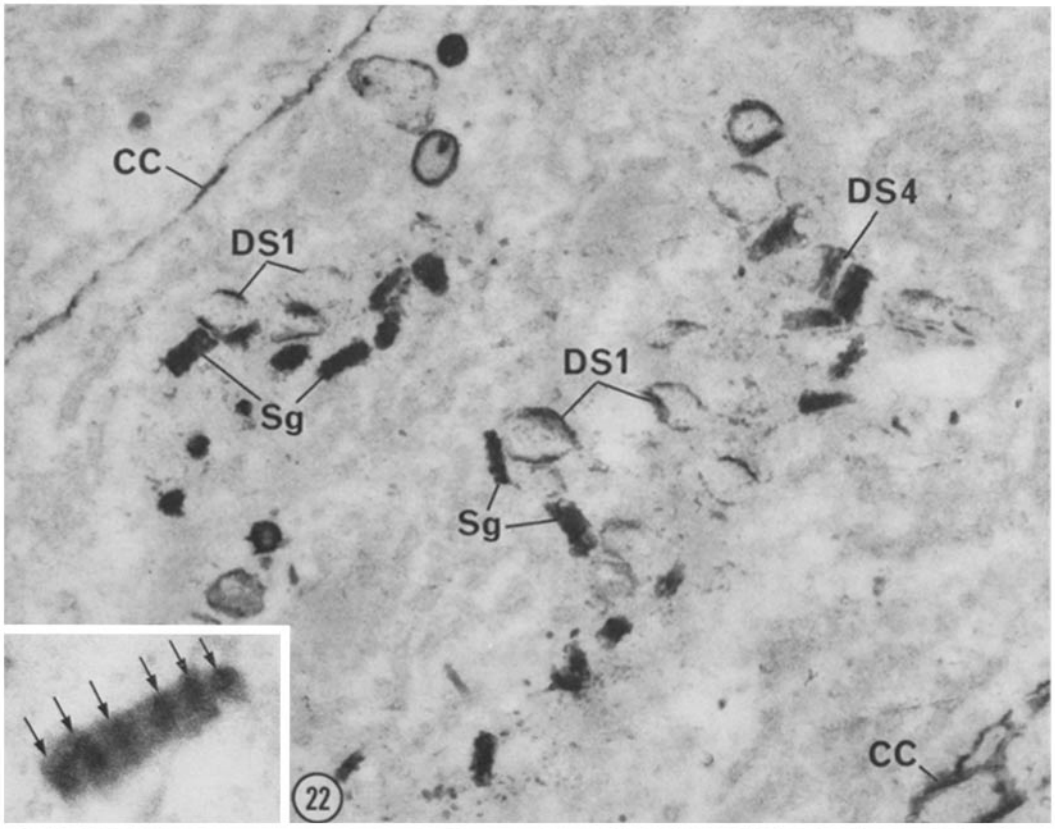
CC
DS1
Sg
DS4
DS1
Sg
CC
22

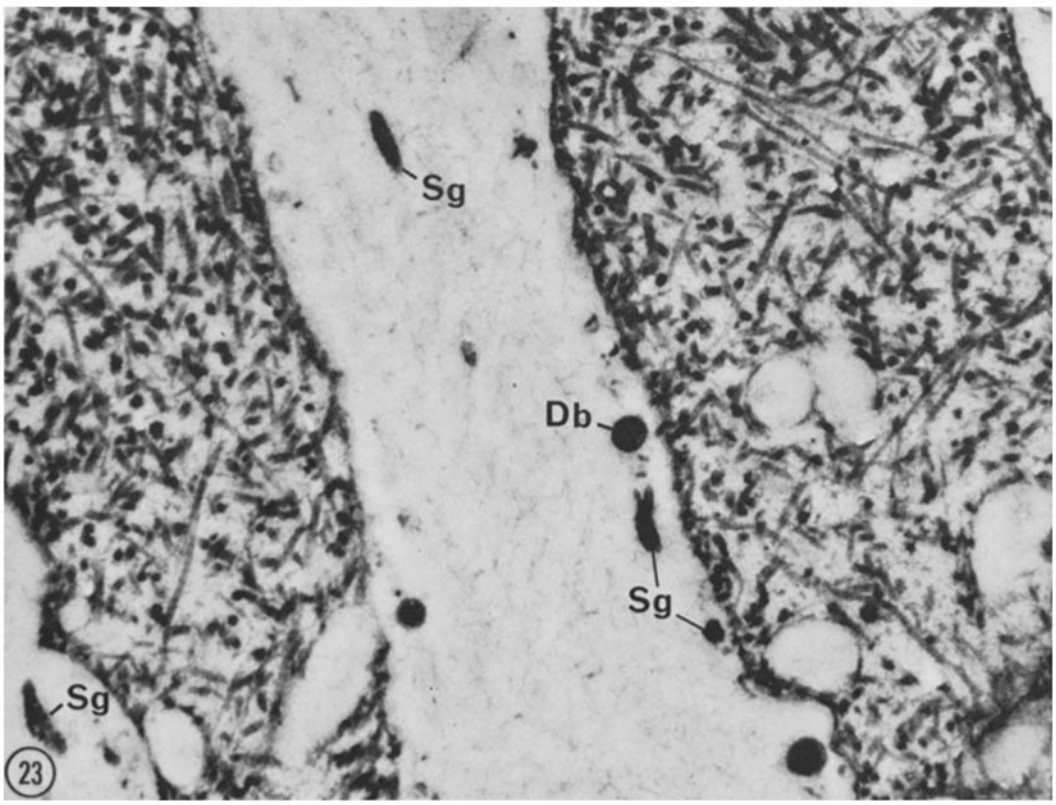
Sg
Db
Sg
Sg
23

threads observed in the cylindrical distensions of saccules described in routinely stained sections. Intense staining was also observed in the elongated profiles corresponding to prosecretory and secretory granules. However, the spherical distensions of Golgi saccules and the cisternae of rough endoplasmic reticulum remained unstained.

In the odontoblast process an intense staining of the content of secretory granules was also noted. From the examination of profiles of granules cut in longitudinal and cross section (Fig. 25), it became apparent that the silver precipitate accumulated over the small bundles of threads making up the condensed aggregates.

In predentin, the silver precipitate accumulated over collagen fibrils which could be seen deep in predentin or within scalloped regions of the plasmalemma (Fig. 25).

Radioautographic Results

LIGHT MICROSCOPY: At 2 min after [^{3}H]-proline administration, silver grains were observed chiefly over the basophilic supranuclear and apical regions (ergastoplasm) of the odontoblast (Fig. 26). In contrast, the number of silver grains over the Golgi region, odontoblast process, predentin, and dentin was not above background. At 10 min, silver grains were observed not only over the ergastoplasm, but also over the Golgi region (Fig. 27). By 20 min, numerous silver grains appeared in clusters over the Golgi region and some were still observed over the ergastoplasm (Fig. 28). At 30 min, the odontoblast process and the proximal predentin became labeled (Fig. 29). At no time were significant numbers of silver grains observed along the lateral borders or the base of the cells. By 4 h, the entire predentin was heavily labeled (Fig. 30). At 30 h, clusters of silver grains were observed as a wide band over the dentin just beyond the predentin-dentin junction (Fig. 31).

Counts of silver grains per unit area (Table I) confirmed that radioactivity was limited to the cells at early time intervals and appeared later in predentin and finally dentin. Graphic representation of these results (Fig. 32) showed a peak in the cells at 30 min, at which time radioactivity also appeared in predentin. At 4 h a peak was observed over predentin and at 30 h radioactivity was over dentin.

The above results are consistent with the notion that synthesis occurs within cells and the product then moves into the predentin matrix where it accumulates. Since no radioactivity was detected between the cells or below the base of the cells, release of radioactivity occurred essentially from the apical processes into the predentin indicating that the cell is well polarized with respect to the site of collagen secretion and that the collagen is secreted in a well-defined location with respect to the cell body.

ELECTRON MICROSCOPY:[1] Radioautographs obtained 2 min after [^{3}H]proline administration

[1] The tissues used for radioautography were fixed with 3% formaldehyde in Sörensen's phosphate buffer. Under these conditions of fixation, entangled threads could be identified in the spherical portions of Golgi saccules and parallel threads in the cylindrical portions, as was the case after glutaraldehyde fixation. However, prosecretory and secretory granules did *not* show the 30-nm electron-opaque particles identified in glutaraldehyde-fixed tissues, although smaller electron-dense particles were dispersed within the granules.

The small size of these electron-dense particles (about 10 nm) precludes the possibility of confusing them with silver grains (about 40 nm).

FIGURES 24 and 25 Portions of odontoblasts embedded in Epon and stained with *silver methenamine*.

FIGURE 24 Silver precipitate accumulates on rodlike structures aggregated within the cylindrical portions of Golgi saccules (*DS4*). Profiles of these rodlike structures in cross section (arrows) also stain. In addition, silver precipitate accumulates within secretory granules (*Sg*). Spherical distensions of Golgi saccules (*DS1*) and flattened portions (*S*) as well as the rER (*rER*) do not stain above background. × 30,000.

FIGURE 25 Portion of an odontoblast process and adjacent predentin matrix depicting the accumulation of silver precipitate within secretory granules (*Sg*). The appearance of granules sectioned longitudinally or in near cross section suggests that the silver accumulates in the parallel threads which they contain. In their staining with silver, these structures resemble the collagen fibrils observed in the dentin matrix. The secretory granules are likely analogous to those identified with phosphotungstic acid (Fig. 23) and conventional electron microscopy (Fig. 19). The cytoplasmic ground substance, bristle-coated vesicles (*Cv*), and interfibrillar matrix material in the predentin do not stain above background. × 30,000.

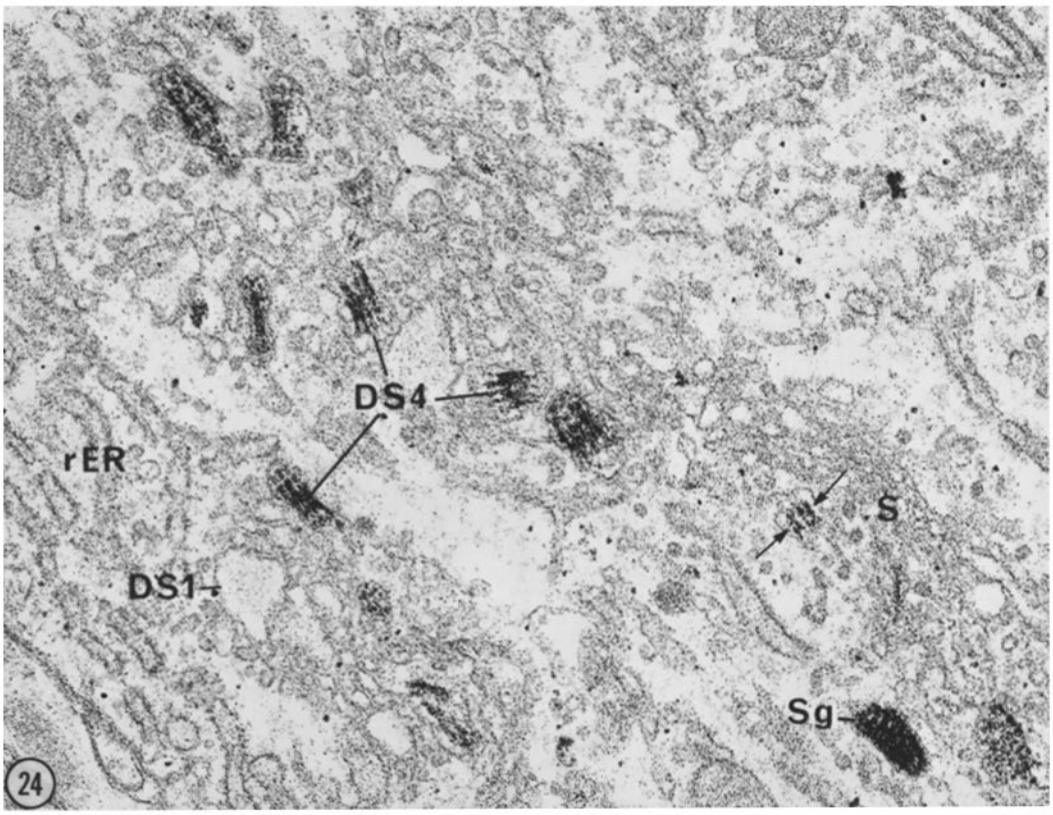
DS4
rER
S
DS1
Sg
24

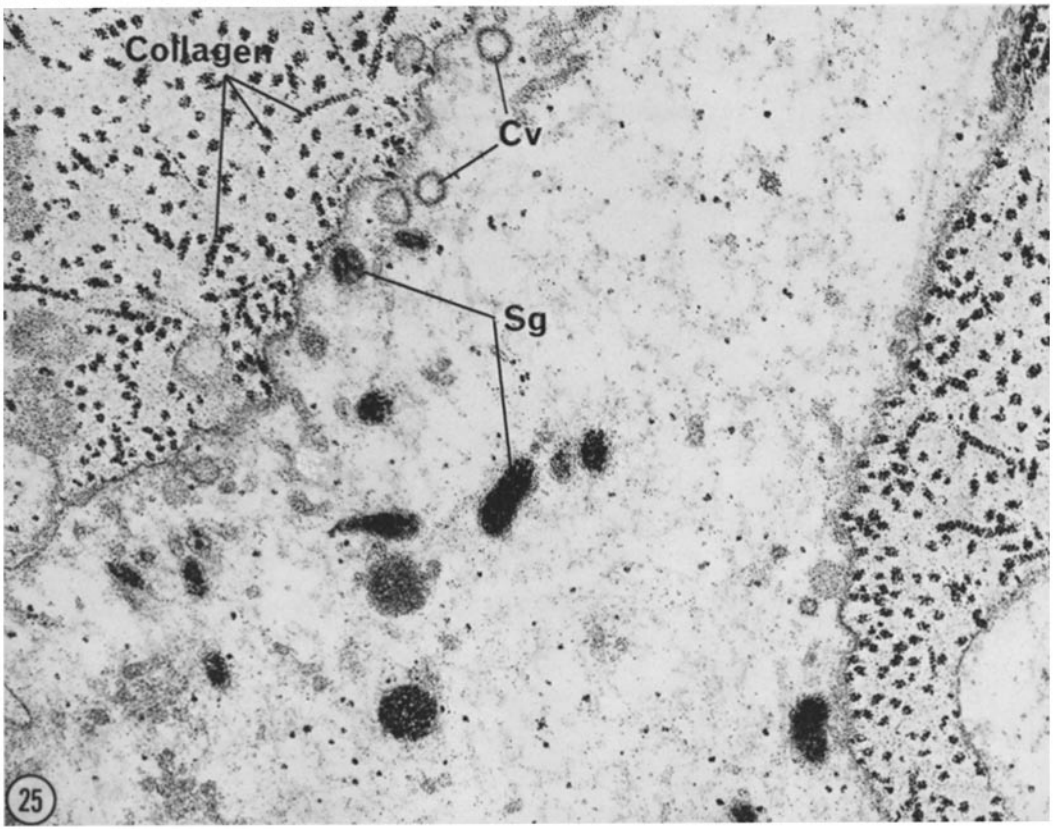
Collagen
Cv
Sg
25

revealed the presence of numerous silver grains over the rough endoplasmic reticulum in all its locations (Figs. 33, 34). A few silver grains were noted over the nucleus and mitochondria, whereas the Golgi apparatus remained unlabeled (Fig. 34).

At 10 min silver grains were present over the spherical portions of Golgi saccules containing entangled threads (Fig. 35, DS1) as well as over profiles of the rough endoplasmic reticulum. Cylindrical portions (DS4) as well as secretory granules were unlabeled. By 20 min, however, silver grains were observed over the cylindrical portions containing parallel threads as well as over prosecretory granules, and less frequently over secretory granules (Fig. 36). By 30 min, clusters of silver grains were present over secretory granules not only in the Golgi region (Fig. 37), but also in the apical portion of the cell (Fig. 38) and the odontoblast process (Fig. 39). In contradistinction, the cytoplasmic ground substance appeared to be free of silver grains.

By 4 h the secretory granules were for the most part unlabeled, but there was an increase in the number of silver grains over the predentin matrix (Fig. 40). Frequently, clusters of silver grains appeared over collagen fibrils that were aligned adjacent to odontoblast processes viewed in tangential section.

The results of electron microscope *quantitation* (Table III) demonstrated at 2 min after [^{3}H]-proline injection that 94% of the silver grains were present over the rough endoplasmic reticulum. Thereafter, the percentage progressively decreased, so that by 4 h very few silver grains remained over this organelle. Concomitantly, there was a progressive increase in the percent silver grains over the Golgi apparatus, reaching a peak at 20 min. Since at that time the two compartments comprised 90% of the silver grains, radioactivity must have passed from the endoplasmic reticulum into the Golgi apparatus.

At 20 min 6% of the silver grains appeared over the secretory granules and at 30 min a peak was reached. Since the percent silver grains peaked at 2 min in the rough endoplasmic reticulum and at 20 min in the Golgi apparatus, the sequence is in support of a Golgi source rather than a rough endoplasmic reticulum source for the radioactivity of secretory granules.

A rise in the percent silver grains over predentin began at 30 min. By 4 h approximately 95% of the silver grains were in this location, indicating that nearly all the cell radioactivity had passed into predentin.

When the quantitation was expressed in terms of *concentration* of radioactivity as determined by dividing the percent grains over a structure by the percent volume occupied by that structure as recorded in Table V (40, 81), the results (Fig. 41) demonstrated peaks occurring successively over

---

FIGURES 26–31 Light microscope radioautographs of odontoblasts, predentin, and dentin from young rats sacrificed at various times after intravenous administration of a single dose of [^{3}H]proline. × 1,000.

FIGURE 26 At 2 min, silver grains are localized chiefly over the ergastoplasm of the odontoblasts (*Od*). The Golgi region, predentin (*Pd*), and dentin (*D*) are not labeled above background (19-day exposure).

FIGURE 27 At 10 min, the silver grains predominate over the ergastoplasm but some are over the lightly stained Golgi region (3-day exposure).

FIGURE 28 At 20 min, some silver grains are present over the ergastoplasm but they now predominate over the Golgi region. Portions of the apical cytoplasm are also labeled, but predentin and dentin are not (3-day exposure).

FIGURE 29 At 30 min, silver grains are present over the proximal predentin and the odontoblast processes. Label persists in the Golgi region (3-day exposure). No accumulation of grains was observed on the pulpal side of the odontoblasts (*Od*) or between the cells at this or other time intervals.

FIGURE 30 At 4 h, label predominates throughout predentin while most of the radioactivity has left the cells. The dentin is unlabeled at this time (3-day exposure).

FIGURE 31 At 30 h, the radioactive band is present over the dentin beyond the predentin-dentin junction due to a gradual transformation of labeled predentin into labeled dentin. A few grains are present in the distal predentin at this time, whereas very little is in proximal predentin and in the cells (3-day exposure).

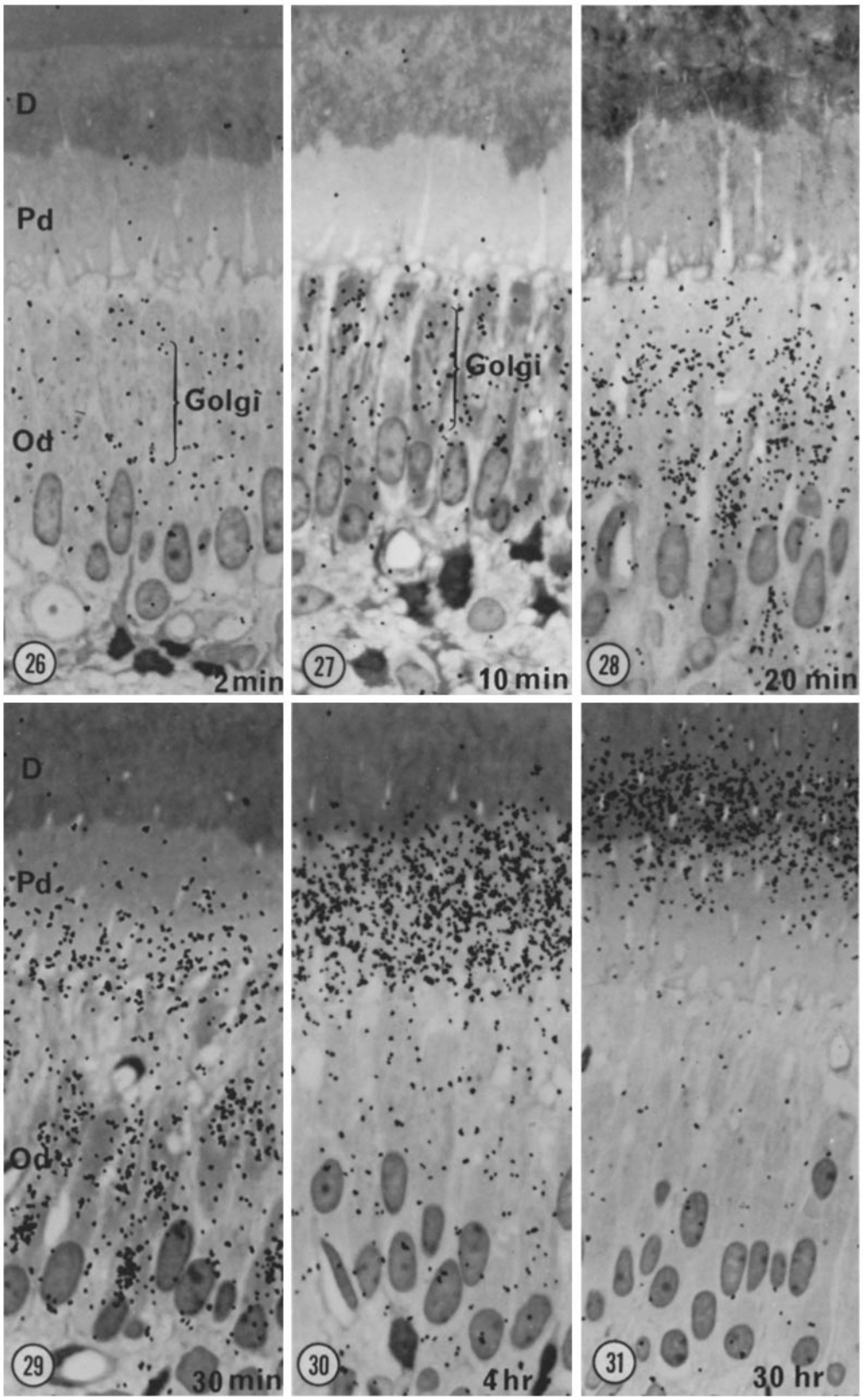
D
Pd
Golgi
Od
26
2 min
Golgi
27
10 min
28
20 min
D
Pd
Od
29
30 min
30
4 hr
31
30 hr

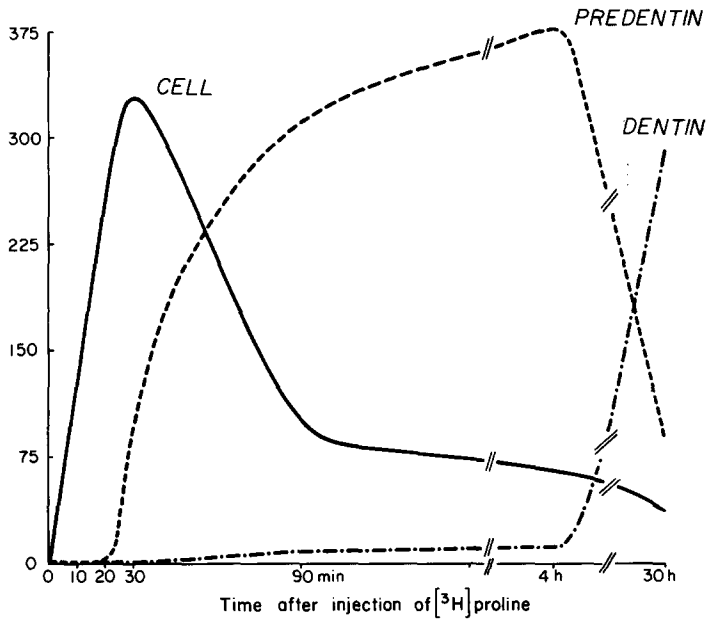

FIGURE 32 Graphic representation of light microscope quantitative radioautography at various time intervals after injection of [^{3}H]proline. The counts of silver grains were taken from Table I; those over cells were obtained by pooling the figures for cytoplasm and odontoblast process and those over predentin by pooling the figures for distal and proximal predentin. The results are consistent with the notion that synthesis occurs within the cells and the product then moves from the cells into the predentin matrix where it accumulates. Release of radioactivity was not detected from the base of the cells or into the extracellular spaces between adjacent cell bodies, but only from the apical processes into predentin, indicating that the collagen precursors formed are secreted in a predictable location from the apical pole of the cell. By 30 h, the radioactivity was markedly decreased in predentin but accumulated in nearby dentin, indicating that during that period of time the predentin had transformed into dentin.

the rough endoplasmic reticulum at 2 min, Golgi apparatus at 20 min, secretory granules at 30 min, and dentin at 4 h. The concentration of radioactivity, which takes into account the volume occupied by each organelle within odontoblasts, a value which did not change with time, strongly suggests sequential passage through each one of these compartments. In particular the high peak over secretory granules at 30 min indicated that, in spite of the relatively small percent silver grains (15%) present, the granules contained a sufficiently high concentration of radioactivity to lead to the conclusion that they are the carriers of the proline-labeled protein from cell to predentin.

FIGURES 33 and 34 Electron microscope radioautographs of supranuclear portions of odontoblasts from animals sacrificed *2 min* after [^{3}H] proline injection. Unless otherwise indicated, these and the following figures (up to Fig. 40) were developed in a solution physical developer.

FIGURE 33 Silver grains appearing as black dots may be seen overlying profiles of cisternae of rough endoplasmic reticulum. There appears to be a preferential localization over the membrane of the endoplasmic reticulum where numerous attached ribosomes may be identified. The nucleus is seen at lower left (4-mo exposure). × 45,000.

FIGURE 34 Silver grains overlay the rough endoplasmic reticulum (left) but not the elements of the Golgi apparatus (right of center). Distended Golgi saccule (*DS1*) and secretory granules (*Sg*) are unlabeled. Elon ascorbic acid development. (2.5-mo exposure). × 27,000.

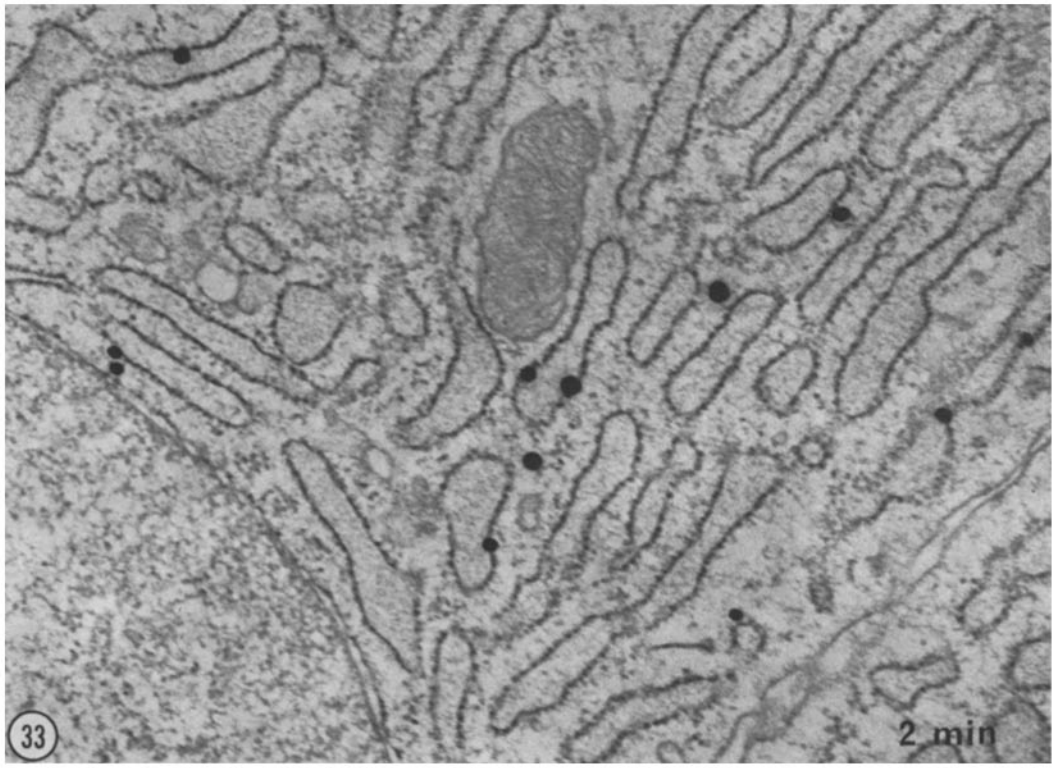
33
2 min

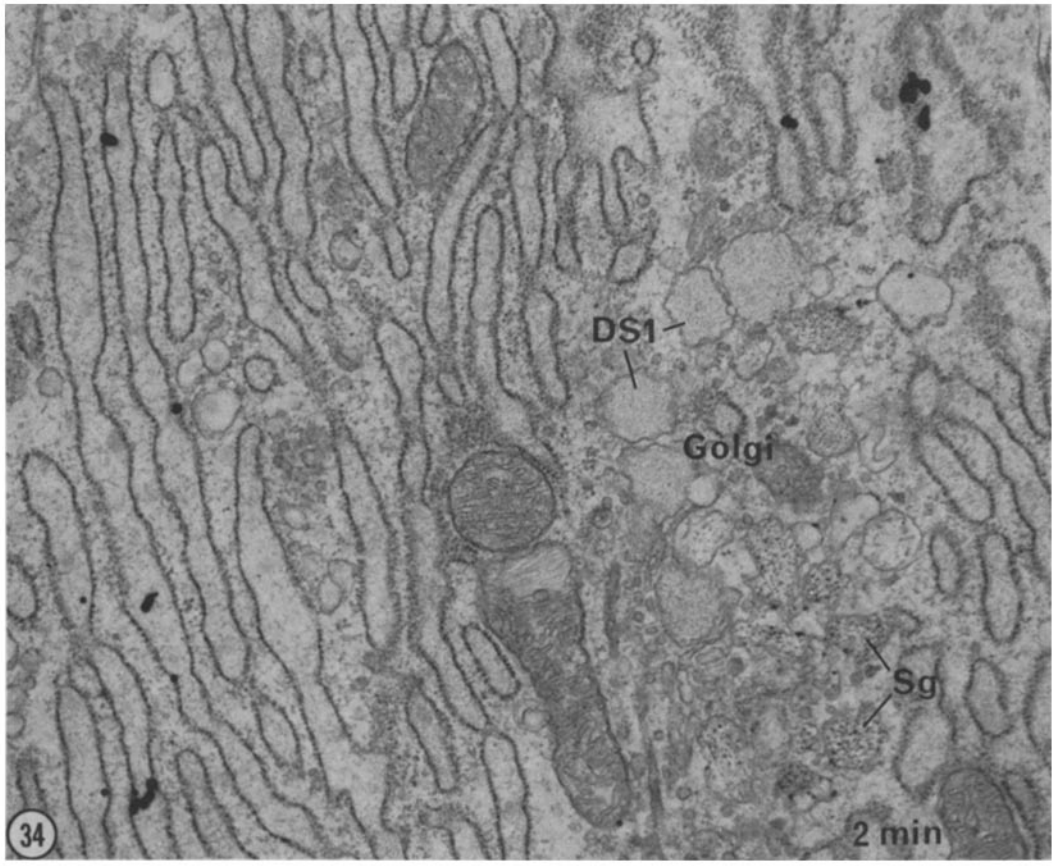
DS1
Golgi
Sg
34
2 min

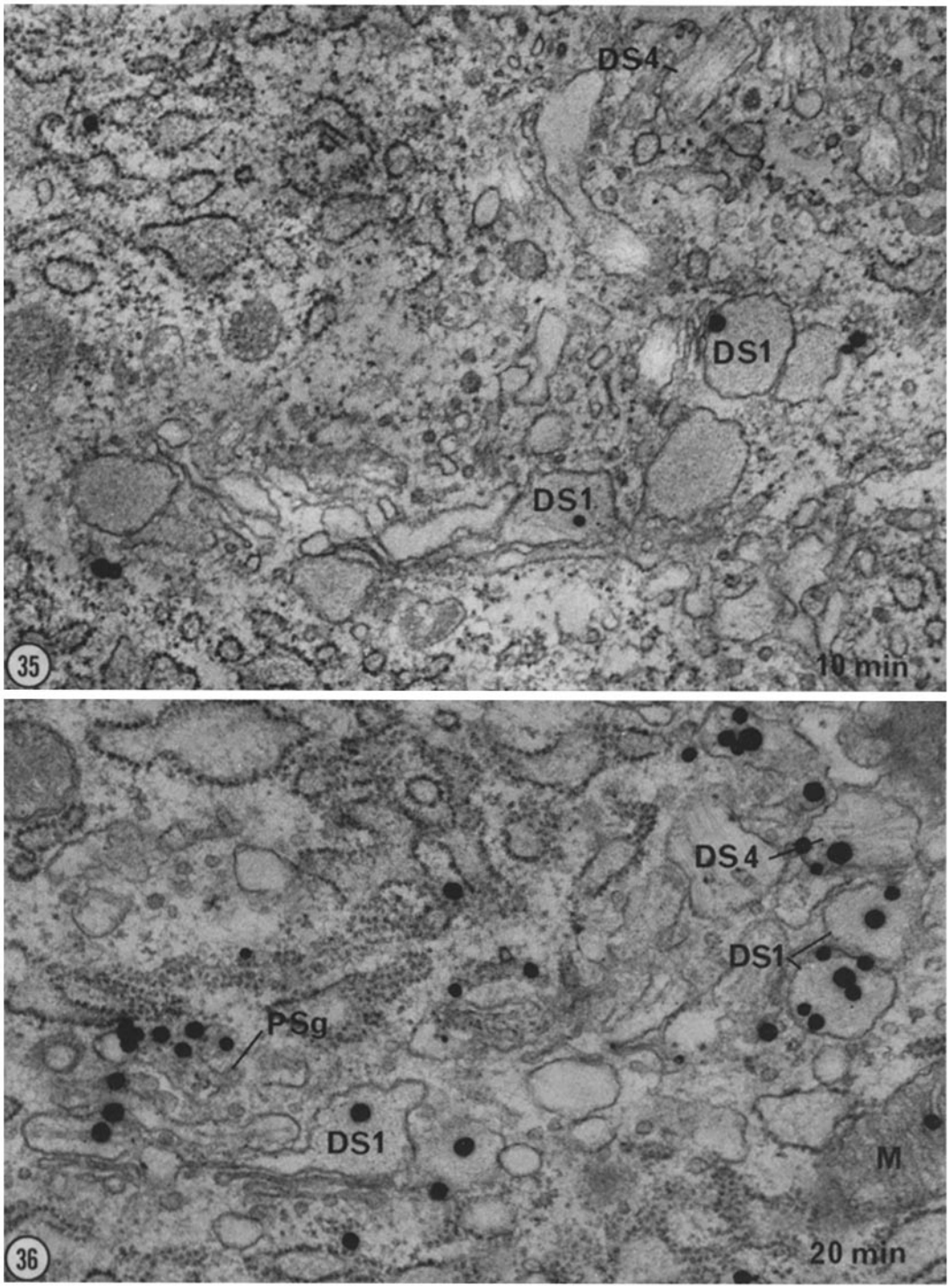

FIGURES 35 and 36 Radioautographs of Golgi regions of odontoblases after [^{3}H]proline injection.

FIGURE 35 Animal sacrificed *10 min* after injection (3-mo exposure). By this time silver grains are found over the spherical portions of Golgi saccules (*DS1*). The cylindrical portions containing parallel threads (*DS4*) are unlabeled at this time. A few silver grains persist over the rough endoplasmic reticulum. × 45,000.

FIGURE 36 Animal sacrificed *20 min* after injection (4-mo exposure). Silver grains may be seen overlying the distended portions (*DS1* and *DS4*) as well as the prosecretory granules (*PSg*). The transfer of label from DS1 to prosecretory granules is attributed to a progressive transformation of the former into the latter. Silver grains are also present over the rough endoplasmic reticulum and a mitochondrion (*M*). × 45,000.

DISCUSSION

Since proline and its derivative hydroxyproline constitute a high proportion (20%) of the amino acid residues of collagen (6), tritium-labeled proline is an ideal tracer to investigate the biosynthesis of this protein. From the data of Butler et al. (6), it was estimated that about 98% of the proline found in incisor dentin is within collagen. Therefore, it may be assumed that nearly all the [^{3}H]-proline which enters dentin is taken up into collagen. It was calculated from the specific activity of the [^{3}H]proline that the 2.5 mCi injected in each animal contained 6.3 μg of proline. Since the concentration of free proline in rat plasma is 43 $\pm$ 4 μg per ml (24), presumably the slow injection of 6.3 μg did not significantly alter the physiological metabolism of proline. The labeling found in odontoblasts soon after [^{3}H]proline injection should identify the sites of uptake of proline into newly formed collagen precursors, i.e. the sites of their synthesis, while the labeling found at later times should reveal the pathway of their intracellular transport.

After intravenous injection of [^{3}H]proline, the radioactivity of the acid-soluble fraction of blood, presumably corresponding to free [^{3}H]proline, was initially high, but declined rapidly so that at 20 min there was less than 20% of the amount detected at 2 min after injection (Fig. 1). This indicated that a pulse of highly radioactive proline was achieved by intravenous injection of the tracer.

Nature of Intracellular Collagen

Collagen fibrils are made up of monomers rereferred to as tropocollagen. A tropocollagen monomer is an asymmetric molecule composed of three polypeptides coiled into a triple helix. The polypeptides, known as alpha chains, are said to be randomly coiled (44), an expression indicating that their shape is variable, whereas the tropocollagen molecule is a rigid rod measuring 1.36 $\times$ 300 nm (3).

Biochemical studies, recently reviewed by Grant and Prockop (22), have clarified the biosynthetic steps in the formation of tropocollagen. The polypeptide chains are first synthesized as pro-alpha chains, which are identical to the alpha chains of tropocollagen (2, 4, 13, 14, 27, 34, 38, 68) except for an extension or "tail piece" of about 13 nm at their NH_2-terminal end (14, 38, 63). Pro-alpha chains are likely to be randomly coiled, like alpha chains.

Eventually three pro-alpha chains join and coil to form a triple helix, referred to as either "transport form" (14, 27, 34) or more commonly "procollagen" (2, 4, 38, 63, 68). Procollagen then is identical to tropocollagen except for the presence of the tail pieces of the three pro-alpha chains at one end of the molecule (14). Consequently procollagen, like tropocollagen, is likely to be in the form of a rigid rod.

While tropocollagen molecules have the ability to self-assemble into collagen fibrils, procollagen cannot do so until the tail pieces are cleaved off (14, 63) by a procollagen peptidase (27). Studies of embryonic tendon fibroblasts indicate that this enzyme is mainly present extracellularly and that the tail piece is removed after the procollagen has been secreted outside the cell (27). Procollagen, then, would be an intracellular precursor form of tropocollagen (14). Since, like tropocollagen, it is rich in proline and hydroxyproline, its passage through the cell may be followed to advantage by radioautography using [^{3}H]proline.

Site of Synthesis

2 min after the injection of [^{3}H]proline, radioactivity was present within the rough endoplasmic reticulum (Figs. 33, 41). This finding is in agreement with those of other investigators who reported that, in radioautographs of various collagen secreting cells, the initial incorporation of [^{3}H]-proline occurs in this organelle (16, 53, 55, 57, 59). Since silver grains were often observed over the cisternal membranes and the associated ribosomes, the synthesis of the pro-alpha chains of dentin collagen probably occurs on membrane-bound ribosomes. This conclusion is in accord with biochemical studies on various cell types that secrete collagen (10, 21, 30, 48).

Passage of Label into the Golgi Apparatus

After their synthesis on ribosomes, the pro-alpha chains were presumably located in the cisternae of the rough endoplasmic reticulum. By 5 min after injection the labeled proline was still restricted to this organelle. By 10 min some label appeared in the Golgi apparatus. By 20 min the percent silver grains reached a peak in this organelle while declining from a 2-min peak in the rough endoplasmic reticulum (Table III, Fig. 41). This indicates that radioactivity passed from the rough endoplasmic

reticulum to the Golgi apparatus, although the possibility that a small fraction of the radioactivity entered the Golgi apparatus directly cannot be ruled out.

At the 10-min interval, radioactivity was present for the most part in the spherical portions of saccules containing entangled threads (Fig. 35); by 20 min label also appeared in the cylindrical portions containing parallel threads (Fig. 36).

Biochemical studies on cultured chick embryo tendon cells have provided evidence that procollagen triple helix formation occurs before secretion into the extracellular matrix and that a large fraction of the intracellular collagen material is in the form of procollagen (28). Where then do the pro-alpha chains transform into procollagen? The pro-alpha chains would be difficult to identify on the basis of length since they are randomly coiled, but they could appear as the threads observed in the cisternae of the rough endoplasmic reticulum or as the fine entangled threads identified in the spherical portions of Golgi saccules.

Hence, the pro-alpha chains could transform into procollagen either within the cisternae of rough endoplasmic reticulum or within Golgi saccules. In the first case, *procollagen molecules* would enter Golgi saccules as entangled threads and would subsequently become organized into parallel threads. In the second case, *pro-alpha chains* would appear as entangled threads in Golgi saccules where they would transform into procollagen molecules appearing as parallel threads.

In either case, the appearance of label at 10 min in the spherical portions of saccules would imply entry from the cisternae of the rough endoplasmic reticulum. This transport may occur by way of the fuzz-coated vesicles and blebs often present in the interval between the cisternae of rough endoplasmic reticulum and the Golgi saccules (Figs. 10, 42). These are referred to as intermediate or transitional vesicles, since they appear analogous to the vesicles which were described in other protein-synthesizing cells (26, 72) and were believed to participate in the transport of protein from the rough endoplasmic reticulum to the Golgi apparatus (26, 72). Another method of transport may be by way of the smooth transitional cisternae of endoplasmic reticulum often found adjacent to the first Golgi saccules (Figs. 7, 9). Either transitional cisternae containing the transported material would transform into Golgi saccules or direct connections between transitional cisternae and the Golgi saccules would enable passage from the rough endoplasmic reticulum to occur. To date, direct communication between the rough endoplasmic reticulum and the Golgi membrane system has not been clearly observed in odontoblasts, but images suggesting such communication have been noted in other cell types (11).

At 20 min after [^{3}H]proline injection label was detected within the cylindrical portions of Golgi saccules containing parallel threads. Since the pulse of labeled proline in the blood was reduced by as much as 80% at 20 min, it is unlikely that the cylindrical portions incorporated a substantial amount of label directly. Hence, the labeled material present in spherical portions must have found its way into the cylindrical portions.

The first possibility was that connections between spherical and cylindrical portions allowed

---

FIGURES 37 and 38 Radioautographs of portions of odontoblasts after [^{3}H]proline injection.

FIGURE 37 Golgi region of an odontoblast from an animal sacrificed 30 min after injection (4-mo exposure). Silver grains predominate over profiles identified as prosecretory (*PSg*) and secretory (*Sg*) granules on one side of the Golgi apparatus. Some silver grains are still present over the rER and the distended portions of saccules (*DS1* and *DS4*). The abundance of grains over the granules suggests that radioactivity is concentrated within them. *Pm*, plasma membrane. × 40,000.

FIGURE 38 Apical region of an odontoblast from an animal sacrificed *30 min* after injection. The distribution of radioactivity is depicted over that area of the cell and the base of the odontoblast process (4-mo exposure). Clusters of silver grains may be seen over the secretory granules (*Sg*) routinely found in this region. A few silver grains are also present over predentin (*Pd*), indicating that labeled collagen precursors have already been deposited there. *Pm*, plasma membrane. *Inset* depicts invagination of the plasmalemma at the base of the odontoblast process. 30 min after [^{3}H]proline injection label is present over the content of that invagination. Moderately electron-dense accumulations are present on the cell surface (compare with Fig. 21). × 40,000. Inset, elon ascorbic acid development. × 60,000.

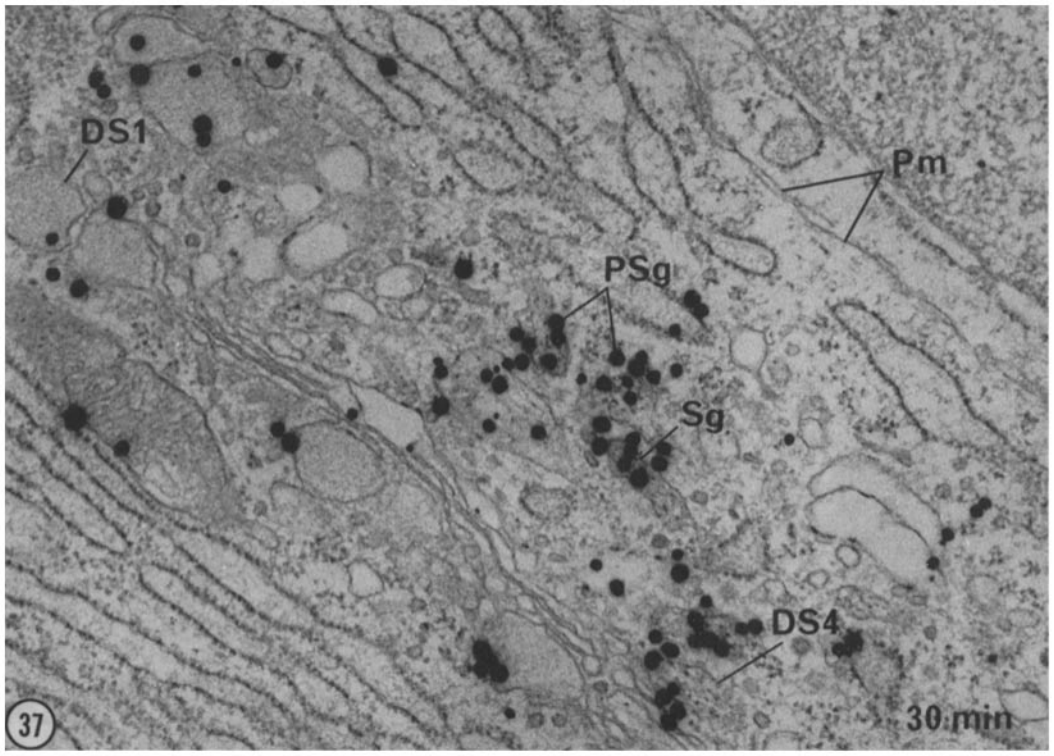
DS1
Pm
PSg
Sg
DS4
37
30 min

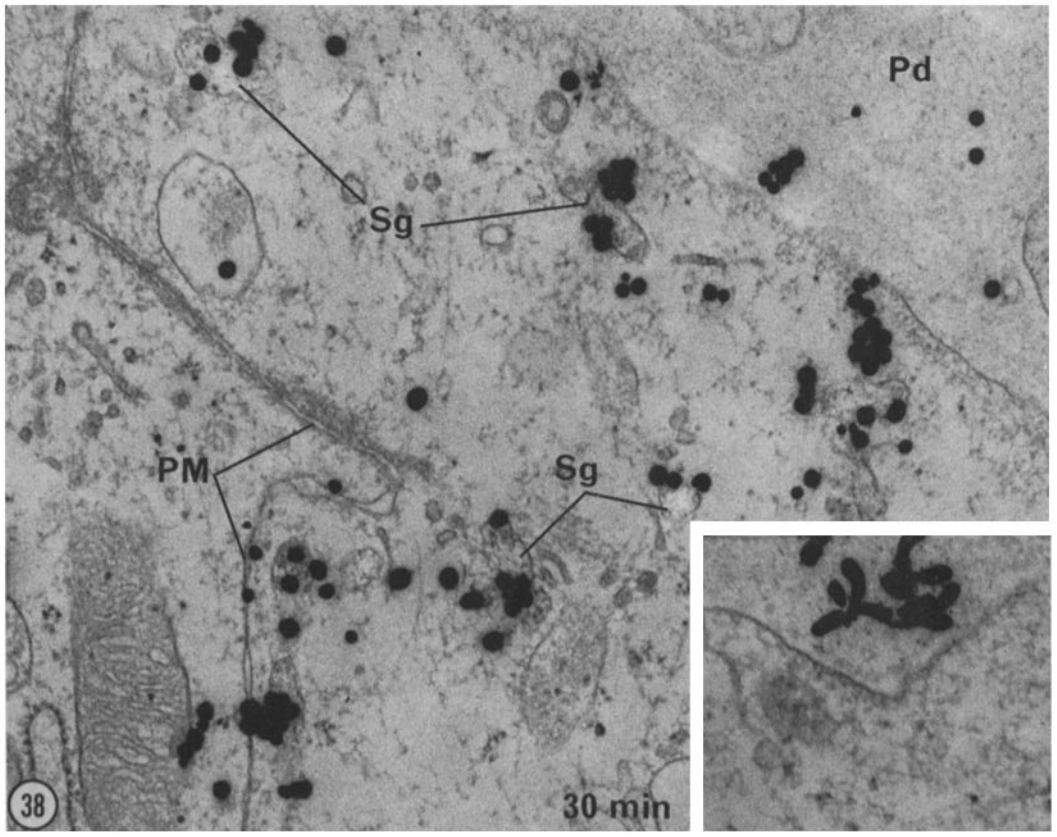
Pd
Sg
PM
Sg
38
30 min

transfer of labeled material. However, such connections have not been seen so far. A more plausible explanation would be that the spherical portions labeled at 10 min transformed into the cylindrical portions labeled at 20 min. Support for this inserpretation comes from the observations illustrated by the sequence depicted in Figs. 11–14 showing transitional stages of the distended Golgi saccules in which the entangled threads become parallel. Since procollagen molecules are likely to be rigid rods, it is tempting to propose that the parallel threads in cylindrical portions correspond to procollagen molecules. The length of the parallel threads (280–350 nm) is in fair agreement with the known length of procollagen molecules (300 nm). The spherical saccules would assume a cylindrical shape to accommodate the rigid parallel molecules of procollagen.

An additional observation was that the "aggregates" of parallel threads showed periodically spaced bands (Fig. 13) which often displayed symmetry (Fig. 14). Such symmetry may indicate that the threads are procollagen molecules aligned parallel in the same manner as the fibrous long spacing type collagen in which tropocollagen molecules are oriented head to tail (25).

CARBOHYDRATE ATTACHMENT TO DENTIN GLYCOPROTEINS: Examination of the histochemical results using the low pH-phosphotungstic acid stain (52) which reliably stains glycoproteins (50) provided some information regarding the stage at which carbohydrates may become associated with proteins to form glycoproteins that are secreted into predentin by odontoblasts. The strong staining observed within cylindrical portions of Golgi saccules (Fig. 22) indicates the presence of carbohydrate in the aggregates of parallel threads. In the spherical portions of saccules containing entangled threads, stain was detected only at the periphery. The entangled threads were unstained as was the content of the cisternae of the rough endoplasmic reticulum, indicating that carbohydrate residues were either absent or present in amounts too small for detection. These results would indicate that the addition of carbohydrate occurs in the Golgi saccules where entangled threads are in the process of being oriented into parallel bundles. Since collagen is known to contain carbohydrate (5, 61) and, indeed, collagen fibrils stain with this method (Fig. 23), it is tempting to suggest that glycosylation occurs concomitantly with or soon after the appearance of parallel procollagen molecules within the Golgi saccules.[2]

SILVER METHENAMINE: Examination of sections stained with silver methenamine revealed that reaction product was present in the parallel threads within the cylindrical portions of Golgi saccules while the material within spherical portions as well as in the rough endoplasmic reticulum was unreactive (Fig. 24). Since collagen fibrils represent a unique structure that combines with

[2] Other sites which stained with low pH-phosphotungstic acid included the dense spherical 30-nm particles present in prosecretory and secretory granules (inset, Fig. 22). These particles may correspond to either a fucose-rich glycoprotein (74) or a phosphoprotein (78) believed to be released into the predentin by secretory granules in odontoblasts. Since the phosphoprotein makes up a large percent of dentin proteins (6) and contains galactose and other sugars (Butler, private communication), it is likely that the particles are composed of phosphoprotein.

FIGURES 39 and 40 Radioautographs of portions of the odontoblast process and adjacent predentin after injection of [^{3}H]proline.

FIGURE 39 Animal sacrificed *30 min* after injection (4-mo exposure). Clusters of silver grains are present over a secretory granule (*Sg*), while the surrounding cytoplasmic ground substance is mostly free of radioactivity. A few silver grains are also present over the collagen-rich predentin; they are not seen over minor branches of odontoblast processes sectioned tangentially (arrowheads). ×30,000.

FIGURE 40 Animal sacrificed *4 h* after injection (4-mo exposure). For the most part silver grains are absent from secretory granules (*Sg*) within the process. Large numbers of silver grains, frequently in clusters, are present over the collagen-rich predentin. In this micrograph, a preferential localization seems to occur over the bundles of collagen fibrils (arrowheads) adjacent to an odontoblast process sectioned obliquely. The collagen fibrils lie close to the cell surface. × 30,000.

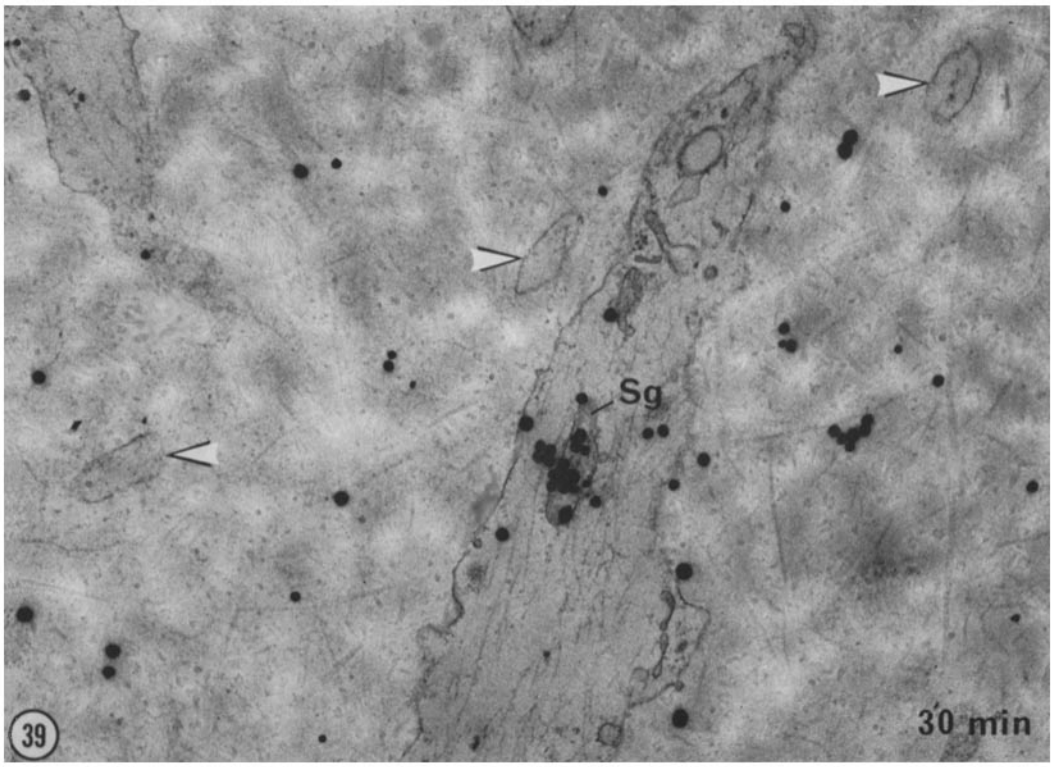
Sg
39
30 min

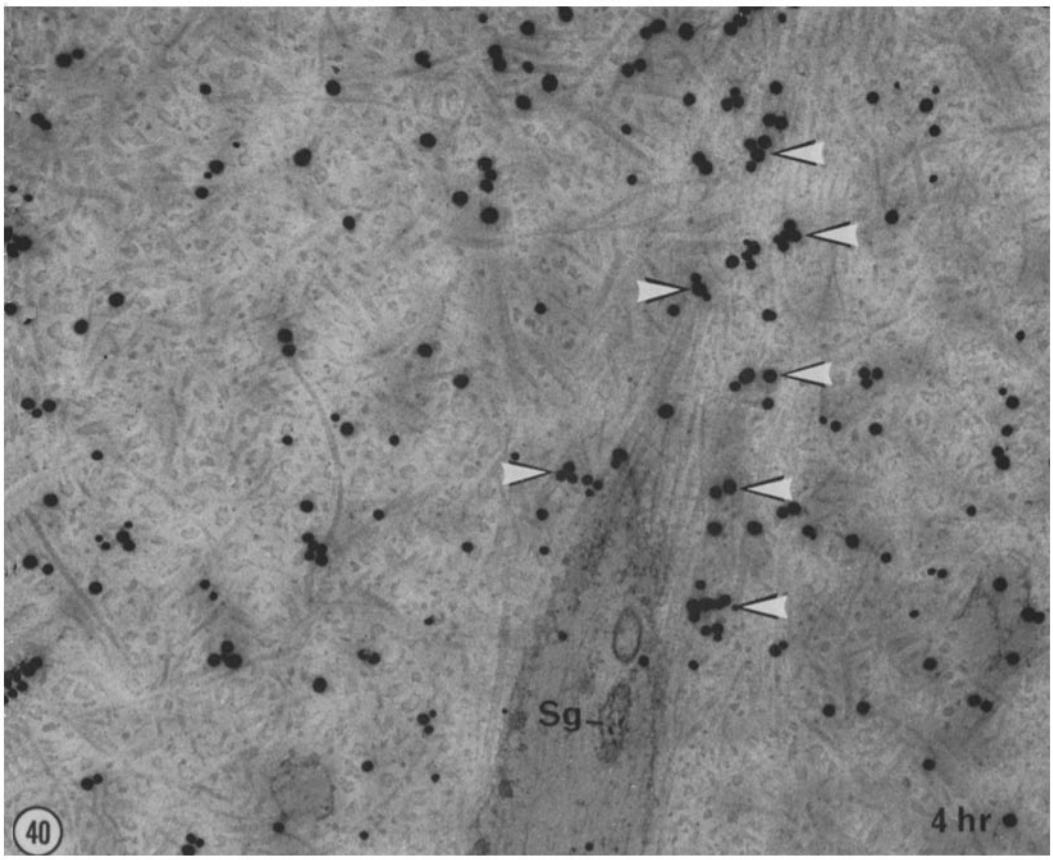
Sg
40
4 hr

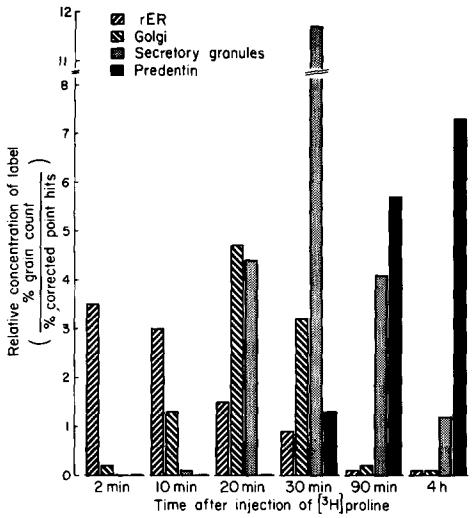

FIGURE 41 Graphic representation of the grain counts over the odontoblast organelles at various times after the injection of [^{3}H]proline. The grain counts are expressed as an index of the relative concentration of label over the rough endoplasmic reticulum, Golgi, secretory granules, and predentin as determined by dividing the percent silver grains over each structure by the percent corrected point hits made over each structure. Under these conditions, label is highly concentrated within elongated secretory granules at 30 min, suggesting that the proline-labeled exportable protein is carried by these granules to predentin.

silver methenamine (51) (Fig. 25), the findings suggest that a collagen-like material forms when entangled threads assemble into parallel aggregates within Golgi saccules. This interpretion lends further support to our contention that the aggregates in the cylindrical saccules correspond to procollagen.

Aldehydes and sulfhydril groups are among the important radicals capable of reducing silver methenamine to metallic silver in sections (45). Since cystine is present only in the 13-nm terminal extension of procollagen (14) and the remaining part of the molecule, like collagen, contains no sulfhydril groups, the staining of collagen fibrils in general and of the parallel threads in particular is likely to be the result of the presence of aldehydic groups. Such groups are known to be acquired by the hydroxylysine residues of procollagen molecules and to be eventually involved in crosslinking (46, 47). Consequently, the histochemical evidence suggests that these aldehydic groups are acquired at a stage which may correspond to the appearance of parallel procollagen molecules.

In summary, the morphological findings and particularly the series depicted in Figs. 11–15, illustrate what is believed to be the sequence of events in the packing of procollagen molecules (threads aligned in parallel). Labeling with [^{3}H]proline not only confirms this sequence of events in the Golgi apparatus, but also indicates that parallel procollagen molecules appear 10–20 min after the initiation of pro-alpha chain synthesis. In addition, the transformation of entangled into parallel threads is associated with the acquisition of staining properties which are characteristic of extracellular collagen fibrils, that is, positive reactions with the low pH-phosphotungstic acid stain and silver methenamine. In the case of odontoblasts, procollagen formation requires approximately 10–20 min. Our conclusions are at variance with biochemical studies on cultured bone cells suggesting that the formation of collagen molecules, including synthesis of pro-alpha chains, coiling into procollagen, and extracellular release, requires only 6 min (68). It should be pointed out that in these biochemical studies there was no evidence that the pro-alpha chains were not included in the collagen fraction. It is possible then that the 6-min intervals corresponded to the time required for pro-alpha chain formation. Procollagen formation would take more time.

Formation of Secretory Granules in the Golgi Region

20 min after [^{3}H]proline injection, label was present not only in cylindrical portions of Golgi saccules, but also in prosecretory granules (Fig. 36). By 30 min, label predominated in prosecretory and secretory granules (Fig. 37). Quantitative methods revealed a sequence of radioactive peak concentrations (Fig. 41) which was in support of the passage of label from the Golgi apparatus into secretory granules. The analysis of fine structure summarized in Fig. 42 and the histochemical demonstration of glycoproteins and aldehydes in the granules as well as in the cylindrical portions of Golgi saccules, but not in the cisternae of rough endoplasmic reticulum (Figs. 22, 24), also support a Golgi origin for secretory granules. Accordingly, it is proposed that cylindrical portions of Golgi saccules bud off from flattened portions and sequentially transform into prosecretory and, later, secretory granules. In the process, saccules would migrate from the proximal to the distal face of the Golgi apparatus. This implies continuous

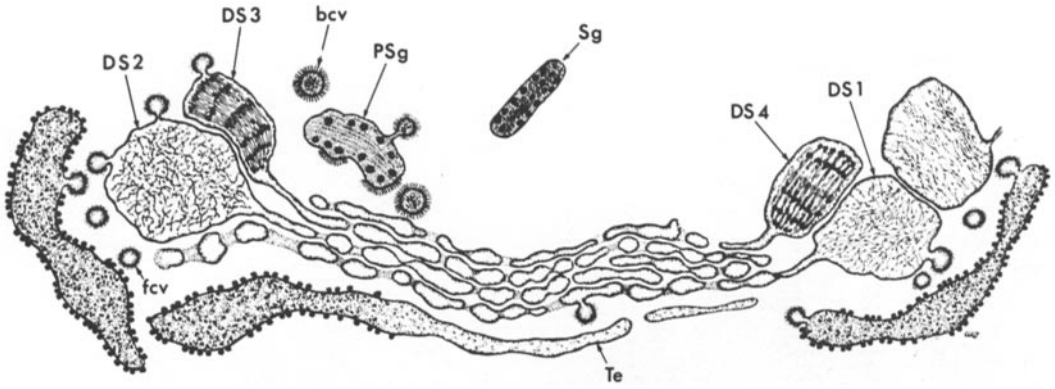

FIGURE 42 Schematic drawing depicting a portion of the Golgi apparatus in the odontoblast and summarizing the presumed sequence of events in the packaging of procollagen into elongated secretory granules. Newly synthesized collagen precursors are transported to the Golgi, either by way of transitional elements (*Te*) or by the fuzz-coated, intermediate vesicles (*fcv*). They are sequestered into the distended spherical portions of Golgi saccules (*DS1, DS2*) where they appear in the form of entangled threads and subsequently into the distended cylindrical portions (*DS3, DS4*) where they appear as parallel threads. The parallel arrangement of the threads is attributed to the rigid moleclules of procollagen. As the cylindrical portion separates from the flattened saccule it carries the aggregate of parallel threads and acquires bristle-coated patches and buds along its surface. At this stage it may be referred to as a prosecretory granule (*PSg*). Bristle-coated vesicles believed to bud off from the prosecretory granules lie free in the cytoplasm (*bcv*). Concomitantly condensation of the procollagen aggregates ensues, with subsequent formation of secretory granules (*Sg*). These migrate to the odontoblast process.

production of new saccules at the proximal face, as suggested in the case of the goblet cell (41).

The transformation of distended portions of Golgi saccules into secretory granules was associated with a decrease in size (Figs. 11–17). Preliminary calculations revealed that this transformation was accompanied by a decrease in surface area from 0.51 to 0.16 μm^2. This decrease implies a loss of membrane. Bristle-coated patches (Fig. 8) and buds (Fig. 7) were regular findings at the surface of prosecretory granules, as were bristle-coated vesicles lying free in the cytoplasm nearby. It is suspected that the bristle-coated vesicles remove material from prosecretory granules and, thereby, participate in the condensation of their content. In addition, they would remove excess membrane. A similar process of membrane removal has been suggested in the transformation of condensing vacuoles into secretory granules in ameloblasts (72).

The formation of prosecretory granules included not only a condensation of the parallel threads within but also the appearance of electron-dense 30-nm particles (Fig. 16). Further condensation of the content of prosecretory granules resulted in the parallel threads no longer being distinguishable in secretory granules (Figs. 8, 17, 19). However, in preparations stained with lead citrate alone (75) or silver methenamine (Figs. 24, 25), there was indication that groups of parallel threads within the aggregate agglomerated into smaller bundles. Each smaller bundle would consist of procollagen molecules.

Migration of Secretory Granules from Golgi Region into Odontoblast Process and Release of their Content into Predentin

Examination of radioautographs at 30 min after [^{3}H]proline injection revealed that numerous secretory granules were labeled in the apical cytoplasm and odontoblast process (Figs. 38, 39). At this time, the concentration of radioactivity was much higher in secretory granules than in any other cell compartment (Fig. 41). Subsequently, the label appeared only in predentin (Fig. 40), never between the cells or at their base. Hence, after their passage to the odontoblast process the secretory granules must have released their content into predentin. This release occurred

by a process of exocytosis, since images of secretory granules in fusion with the plasma membrane of the odontoblast processes were encountered (Figs. 20, 21) (75). Such images were not observed along the lateral and basal membranes of the cell.

An objection to the role of secretory granules in the transport of collagen precursors has been that profiles of granules were not always a conspicuous component in collagen-secreting cells (7, 23, 53, 57) as they are in other secretory cells such as the pancreas and, therefore, could only play a minor role, if any, in collagen formation. Since there was rapid passage of labeled proline from the cell into predentin without indication of cell storage (Fig. 32), the paucity of secretory granules can be explained by the rapidity of their migration and of the release of their content, so that the life of the granules would be short and few would be observed at any one time.

It is important to consider whether procollagen can leave the cell by any pathway other than the secretory granules. As pointed out by others (19, 43, 53, 65, 71), the rough endoplasmic reticulum is absent from the odontoblast process and cell apex in contact with the predentin into which secretion occurs (Fig. 18). Consequently, the rough endoplasmic reticulum could not contribute its contents to the extracellular matrix by fusion with the plasma membrane as suggested by some authors (57). Moreover, there was no indication that any structure other than secretory granules, e.g. cytoplasmic ground substance (53, 59), transitional elements derived from the rough endoplasmic reticulum (20, 57) or bristle-coated vesicles (19), transported proline-labeled protein to the extracellular matrix. We concluded that the secretory granules represent the only pathway for procollagen transport and secretion in odontoblasts.

Radioautographic observations on *osteoblasts* after injection of labeled proline indicate that, in these cells too, secretory granules transport procollagen molecules from the Golgi apparatus to the cell surface (79).

The suggestion that secretory granules participate in the elaboration of collagen in various cell types has already been made by previous investigators (20, 39, 55, 60, 66, 75, 80). The present study extends their findings and provides cytological details of secretory granule formation and of the transport and release of procollagen.

Radioautographic studies using labeled precursors other than [^{3}H]proline, revealed that label was transported from the odontoblast to predentin by the secretory granules. This was demonstrated after injection of the glycoprotein precursor, [^{3}H]fucose (74), the mucopolysaccharide precursor, [^{35}S]sulfate (73), and two phosphoprotein precursors, [^{33}P]phosphate and [^{3}H]serine (78). These observations indicate that secretory granules transport not only collagen precursors, but also phosphoprotein as well as carbohydrates.

Since secretory granules release their contents by exocytosis, the membrane of the granule must be incorporated into the membrane of the odontoblast process and thus contribute a substantial amount of new membrane. Perhaps the excess membrane is disposed of by the large bristle-coated vesicles frequently seen adjacent to (Figs. 6, 18) or confluent with the plasma membrane of the process.

Transformation of Procollagen into Tropocollagen within Predentin

Based on the results of the present study, there seems little reason to question the role of the secretory granules in the intracellular transport of procollagen. What remains to be documented, however, are the steps which occur in the transformation of procollagen into tropocollagen and subsequently into collagen fibrils.

Biochemical studies on embryonic tendon fibroblasts indicate that the conversion of procollagen to tropocollagen is an extracellular event (27, 28) requiring enzymatic cleavage of the NH_2-terminal piece of procollagen (27). This conversion would occur very rapidly since very little procollagen is detectable in the extracellular matrix by chemical means (27). Such a conclusion is borne out by our electron microscope observations of numerous collagen fibrils in predentin. In addition, our radioautographic observations indicate that label spreads quickly into predentin once it is released from the secretory granules. Presumably, the newly formed tropocollagen molecules scatter and rapidly polymerize into collagen fibrils.

In the predentin matrix, at least two types of structures have been observed which might correspond to steps in the transformation of procollagen to tropocollagen. First, invaginations of the plasmalemma (Fig. 21) which may be labeled with [^{3}H]-proline (Fig. 38, inset) were encountered with sufficient frequency to account for the release of procollagen from secretory granules by exocytosis. Adjacent to the cell surface within the concavities,

moderately electron-dense elements were present in regular array within a pale staining area (Fig. 21). It is assumed that these elements correspond to the newly released content of secretory granules and, since they are observed in all degrees of density, that they are gradually dissociated to become part of predentin matrix. On the other hand, it is not known whether these elements represent aggregates of procollagen molecules or the electron-dense particles released from secretory granules.

Elements of a second type which may be considered as a possible step in the transformation of procollagen to tropocollagen are those which were observed either deep in predentin or adjacent to the cell surface and display a crossbanding pattern (Fig. 18, inset). These bear structural similarities to the Golgi aggregates (Fig. 14). Although these elements have previously been observed in predentin matrix (69), they are uncommon and usually appear in localized areas. If they represent procollagen aggregates, for some unknown reasons they have escaped the effect of procollagen peptidase. The possibility that they correspond to reaggregated forms of procollagen and/or tropocollagen which, because of their symmetry, would be composed of molecules aligned head to tail must also be considered.

Collagen fibrils in distal predentin were thicker and more numerous than the newly formed fibrils in proximal predentin. While new fibrils are added to proximal predentin, the older fibrils enlarge as they gradually become part of distal predentin. The enlargement may be attributed to fibril cross-linking, which is known to proceed for some time after the initial deposition of collagen (1, 46, 49). Accompanying this, is a decrease in interfibrillar material (Figs. 4, 18), the removal of which may occur by the bristle-coated vesicles (18, 58) seen along the inner surface of the processes.

Finally, the collagen fibrils at the junction between predentin and dentin (Fig. 4) acquire a network of filaments and small electron-dense particles on their surface (78). Radioautographic studies have shown that this is also the site where minerals are deposited (36) and where a phosphoprotein accumulates (78). The fine threads and/or dense particles appearing on collagen fibrils may represent the morphological counterparts of the phosphoprotein and may play a role in mineralization (78).

CONCLUSION

Several approaches have been used to identify the steps in the elaboration of collagen by odontoblasts. In a previous report it was noted, after staining sections with lead citrate alone, that the collagen fibrils of predentin appeared electron lucent and that, in the odontoblasts, electron-lucent material was observed within the cylindrical portions of Golgi saccules and secretory granules, but notithin the rough endoplasmic reticulum, w or the cytogel (75). Similarly, using the silver methenamine technique, which stains collagen fibrils fairly specifically (Fig. 25) and the low pH-phosphotungstic acid technique which also stains collagen fibrils (Fig. 23), only the contents of cylindrical Golgi portions and secretory granules were stained (Figs. 22, 24). These results suggested that a collagen-like material was present within odontoblasts but was restricted to the cylindrical Golgi portions and the secretory granules.

The study of fine structure added further information about the contents of these two components. The cylindrical portions were found to contain parallel threads which were about the same length as collagen molecules and were responsible for the reactions described above. Images depicting gradual transitions between spherical portions containing entangled threads and cylindrical portions containing parallel threads suggested that the latter arose from the former (Figs. 11–13). Moreover, cylindrical portions appeared to give rise to the secretory granules (Figs. 13–17) in which the parallel threads were closely packed and indistinct but reacted positively to the techniques mentioned above. The secretory granules were also present in cell apex and process and were observed in fusion with the plasmalemma of the process indicating that their contents were released into predentin.

The sequence of events suggested by these observations was scrutinized first by examination and secondly by quantitation of radioautographs after [^{3}H]proline injection. First, the appearance of silver grains over the various cell organelles at different times after injection (Figs. 33–40), that is, at 2 min over the rough endoplasmic reticulum, at 10 min over spherical portions of the Golgi apparatus, at 20 min over cylindrical portions, and at 30 min over secretory granules and predentin, indicated that a proline-labeled protein, presumed to be a precursor of collagen, was synthesized in the rough endoplasmic reticulum,

passed into the Golgi apparatus, and, from there, into secretory granules and then predentin. Secondly, quantitation of radioactivity concentration (Fig. 41) showed a succession of radioactive peaks in the following order: (*a*) in the rough endoplasmic reticulum at the earliest times, 2 min, (*b*) in the Golgi apparatus at 20 min, (*c*) in the secretory granules at 30 min, and (*d*) in predentin at 4 h. Despite the difficulties presented by inadequate chase conditions in studies using live animals, the high concentration of label in secretory granules at 20 and 30 min suggested that they were the carriers of radioactivity from the Golgi apparatus to predentin.

Although the quantitative results alone do not preclude the possibility that the radioactivity bypassed the Golgi apparatus, the evidence gathered from the various approaches together suggests a sequence of events which requires passage through this organelle. After their synthesis in the rough endoplasmic reticulum, the initial precursors of collagen find their way into the spherical portions of Golgi saccules. As the spherical portions transform into cylindrical portions, the content becomes a parallel array of threads possessing collagen-like properties and presumed to consist of procollagen. The cylindrical saccules bud off from the Golgi apparatus to form secretory granules which also contain collagen-like material (procollagen). This is carried to the cell surface by the secretory granules for release into predentin.

The same techniques applied to the study of the osteoblasts of alveolar bone have yielded preliminary results which suggest the same sequence of events as in odontoblasts: initial synthesis in the rough endoplasmic reticulum, assembly of parallel threads with collagen-like properties within the Golgi apparatus, and transport of this material by secretory granules for release into prebone (79).

It is proposed that the steps in the elaboration of collagen in odontoblasts and osteoblasts provide a model applicable to other types of collagen-secreting cells.

The assistance of Dr. Beatrix Kopriwa in the preparation of radioautographs is gratefully acknowledged. We are indebted to Drs. W. T. Butler and B. R. Olsen for discussions on the biosynthetic steps of collagen synthesis.

This work is taken from a thesis submitted by the senior author, Melvyn Weinstock, in partial fulfillment of the requirements for the degree of Doctor of Philosophy of McGill University. Preliminary reports of this work have been presented (76, 77).

This work was supported by grants from the Medical Research Council of Canada. Dr. Melvyn Weinstock is recipient of a Medical Research Council fellowship.

Received for publication 1 February 1973, and in revised form 25 September 1973.

REFERENCES

1. Bailey, A. J., C. M. Peach, and L. J. Fowler. 1970. The biosynthesis of intermolecular crosslinks in collagen. *In* Chemistry and Molecular Biology of the Intercellular Matrix. E. A. Balazs, editor. Academic Press, Inc., New York. 1.
2. Bellamy, G., and P. Bornstein. 1971. Evidence for procollagen, a biosynthetic precursor of collagen. *Proc. Natl. Acad. Sci. U.S.A.* **68**:1138.
3. Boedtker, H., and P. Doty. 1956. The native and denatured states of soluble collagen. *J. Am. Chem. Soc.* **78**:4267.
4. Bornstein, P., K. Von Der Mark, A. W. Wyke, H. P. Ehrlich, and J. M. Monson. 1972. Characterization of the pro-alpha 1 chain of procollagen. *J. Biol. Chem.* **247**:2808.
5. Butler, W. T., and L. W. Cunningham. 1966. Evidence for the linkage of a disaccharide to hydroxylysine in tropocollagen. *J. Biol. Chem.* **241**:3882.
6. Butler, W. T., J. E. Finch, Jr., and C. V. Desteno. 1972. Chemical character of proteins in rat incisors. *Biochim. Biophys. Acta.* **257**:167.
7. Cameron, D. A. 1961. The fine structure of osteoblasts in the metaphysis of the tibia of the young rat. *J. Biophys. Biochem. Cytol.* **9**:583.
8. Carneiro, J., and C. P. Leblond. 1959. Role of osteoblasts and odontoblasts in secreting the collagen of bone and dentin, as shown by radioautography in mice given tritium-labeled glycine. *Exp. Cell Res.* **18**:291.
9. Chalkley, H. W. 1943. Method for the quantitative morphologic analysis of tissues. *J. Natl. Cancer Inst.* **4**:47.
10. Chvapil, M., and J. Hurych. 1968. Control of collagen biosynthesis. *Int. Rev. Connect. Tissue Res.* **4**:67.
11. Claude, A. 1970. Growth and differentiation of cytoplasmic membranes in the course of lipoprotein granule synthesis in the hepatic cell. I. Elaboration of elements of the Golgi complex. *J. Cell Biol.* **47**:745.

12. COOPER, G. W., and D. J. PROCKOP. 1968. Intracellular accumulation of protocollagen and extrusion of collagen by embryonic cartilage cells. *J. Cell Biol.* **38**:523.
13. DEHM, P., and D. J. PROCKOP. 1971. Synthesis and extrusion of collagen by freshly isolated cells from chick embryo tendon. *Biochim. Biophys. Acta.* **240**:358.
14. DEHM, P., S. A. JIMENEZ, B. R. OLSEN, and D. J. PROCKOP. 1972. A transport form of collagen from embryonic tendon: electron microscopic demonstration of an NH_2-terminal extension and evidence suggesting the presence of cystine in the molecule. *Proc. Natl. Acad. Sci. U.S.A.* **69**:60.
15. EASTOE, J. E. 1967. Chemical organization of the organic matrix of dentin. *In* Structure and Chemical Organization of Teeth. A. E. W. Miles, editor. Academic Press, Inc., New York. 2.
16. FRANK, R. M 1970. Étude autoradiographique de la dentinogenèse en microscopie électronique à l'aide de la proline tritiée chez le chat. *Arch. Oral Biol.* **15**:583.
17. FRANK, R. M., and P. FRANK. 1969. Autoradiographie quantitative de l'osteogenèse en microscope électronique à l'aide de la proline tritiée. *Z. Zellforsch. Mikrosk. Anat.* **99**:121.
18. FRIEND, D. S., and M. G. FARQUHAR. 1967. Functions of coated vesicles during protein absorption in the rat vas deferens. *J. Cell Biol.* **35**:357.
19. GARANT, P. R., G. SZABO, and J. NALBANDIAN. 1968. The fine structure of the mouse odontoblast. *Arch. Oral Biol.* **13**:857.
20. GOLDBERG, B., and H. GREEN. 1964. An analysis of collagen secretion by established mouse fibroblast lines. *J. Cell Biol.* **22**:227.
21. GOULD, B. S. 1968. Collagen biosynthesis. *In* Treatise on Collagen. B. S. Gould, editor. Academic Press, Inc., New York. 2/A.
22. GRANT, M. E., and D. J. PROCKOP. 1972. The biosynthesis of collagen. *New Engl. J. Med.* **286**:194.
23. GREENLEE, T. K., JR., and R. ROSS. 1967. The development of the rat flexor digital tendon, a fine structure study. *J. Ultrastruct. Res.* **18**:354.
24. HENDERSON, L. M., P. E. SCHURR, and C. A. ELVEHJEM. 1949. The influence of fasting and nitrogen deprivation on the concentration of free amino acids in rat plasma. *J. Biol. Chem.* **177**:815.
25. HODGE, A. J. 1967. Structure at the electron microscope level. *In* Treatise on Collagen. G. N. Ramachandran, editor. Academic Press, Inc., New York. 1.
26. JAMIESON, J. D., and G. E. PALADE. 1967. Intracellular transport of secretory proteins in the pancreatic exocrine cell. I. Role of the peripheral elements of the Golgi complex. *J. Cell Biol.* **34**:577.
27. JIMENEZ, S. A., P. DEHM, and D. J. PROCKOP. 1971. Further evidence for a transport form of collagen: its extrusion and extracellular conversion to alpha chains in embryonic tendon. *FEBS (Fed. Eur. Biochem. Soc.) Lett.* **17**:245.
28. JIMENEZ, S. A., P. DEHM, B. R. OLSEN, and D. J. PROCKOP. 1973. Intracellular collagen and protocollagen from embryonic tendon cells. *J. Biol. Chem.* **248**:720.
29. KARNOVSKY, M. J. 1965. A formaldehyde-glutaraldehyde fixative of high osmolality for use in electron microscopy. *J. Cell Biol.* **27**:137A.
30. KERWAR, S. S., L. D. KOHN, C. M. LAPIERE, and H. WEISSBACK. 1972. In vitro synthesis of procollagen on polysomes. *Proc. Natl. Acad. Sci. U.S.A.* **69**:2727.
31. KOPRIWA, B. M. 1973. A reliable, standardized method for electron microscope radioautography. *Histochemie.* **37**:1.
32. KOPRIWA, B. M. 1967. A semiautomatic instrument for the radioautographic coating technique. *J. Histochem. Cytochem.* **14**:923.
33. KOPRIWA, B. M., and C. P. LEBLOND. 1962. Improvements in the coating technique of radioautography. *J. Histochem. Cytochem.* **10**:269.
34. LAYMAN, D. L., E. B. MCGOODWIN, and R. G. MARTIN. 1971. The nature of the collagen synthesized by cultured human fibroblasts. *Proc. Natl. Acad. Sci. U.S.A.* **68**:454.
35. LEBLOND, C. P. 1963. Elaboration of dentinal collagen in odontoblasts as shown by radioautography after injection of labeled glycine and proline. *Ann. Histochim.* **8**:43.
36. LEBLOND, C. P., L. F. BELANGER, and R. C. GREULICH. 1955. Formation of bones and teeth as visualized by radioautography. *Ann. N. Y. Acad. Sci.* **60**:630.
37. LEDUC, E. H., and W. BERNHARD. 1967. Recent modifications of the glycol methacrylate embedding procedure. *J. Ultrastruct. Res.* **19**:196.
38. LENAERS, A., M. ANSAY, B. V. NUSGENS, and C. M. LAPIERE. 1971. Collagen made of extended alpha-chains, procollagen, in genetically-defective dermatosparaxic calves. *Eur. J. Biochem.* **23**:533.
39. MOVAT, H. Z., and N. V. P. FERNANDO. 1962. The fine structure of connective tissue. I. The fibroblast. *Exp. Mol. Pathol.* **1**:509.
40. NADLER, N. J. 1971. The interpretation of grain counts in electron microscope radioautography. Appendix to the article by A.

Haddad, M. Smith, A. Herscovics, N. J. Nadler, and C. P. Leblond. *J. Cell Biol.* **49:** 877.

41. Neutra, M., and C. P. Leblond. 1966. Synthesis of the carbohydrate of mucus in the Golgi complex as shown by electron microscope radioautography of goblet cells from rats injected with glucose-H^3. *J. Cell Biol.* **30:**119.
42. D. B. Nichols, H. Cheng, and C. P. Leblond. 1973. Shape and argentaffinity of the granules in the entero-endocrine cells of the mouse small intestine. Submitted for publication.
43. Nylen, M. U., and D. B. Scott. 1958. An electron microscopic study of the early stages of dentinogenesis. *Public Health Serv. Publ. (Wash.)* **613:**1.
44. Öbrink, B. 1972. Non-aggregated tropocollagen at physiological pH and ionic strength. *Eur. J. Biochem.* **25:**563.
45. Pickett-Heaps, J. D. 1967. Preliminary attempts at ultrastructural polysaccharide localization in root tip cells. *J. Histochem. Cytochem.* **15:**442.
46. Piez, K. A. 1968. Crosslinking of collagen and elastin. *Annu. Rev. Biochem.* **37:**547.
47. Piez, K. A. 1970. Biosynthesis of the alpha chains of collagen. *J. Cell Physiol.* **76:**389.
48. Prockop, D. J. 1970. Intracellular biosynthesis of collagen and interactions of protocollagen proline hydroxylase with large polypeptides. *In* Chemistry and Molecular Biology of the Intercellular Matrix. E. A. Balazs, editor. Academic Press, Inc., New York. 1.
49. Ramachandran, G. N. Structure of collagen at the molecular level. *In* Treatise on Collagen. G. N. Ramachandran, editor. Academic Press, Inc., New York. 1.
50. Rambourg, A. 1971. Morphological and histochemical aspects of glycoproteins at the surface of animal cells. *Int. Rev. Cytol.* **31:**57.
51. Rambourg, A., and C. P. Leblond. 1967. Electron microscope observations on the carbohydrate-rich cell coat present at the surface of cells in the rat. *J. Cell Biol.* **32:**27.
52. Rambourg, A., W. Hernandez, and C. P. Leblond. 1969. Detection of complex carbohydrates in the Golgi apparatus of rat cells *J. Cell Biol.* **40:**395.
53. Reith, E. J. 1968. Collagen formation in developing molar teeth of rats. *J. Ultrastruct. Res.* **21:**383.
54. Reith, E. J. 1968. Ultrastructural aspects of dentinogenesis. *In* Dentin and Pulp: Their Structure and Reactions. N. B. B. Symons, editor. E. & S. Livingstone Ltd., Edinburgh.
55. Revel, J. P., and E. D. Hay. 1963. An autoradiographic and electron microscopic study of collagen synthesis in differentiating cartilage. *Z. Zellforsch. Mikrosk. Anat.* **61:**110.
56. Reynolds, E. S. 1963. The use of lead citrate at high pH as an electron-opaque stain in electron microscopy. *J. Cell Biol.* **17:**208.
57. Ross, R., and E. P. Benditt. 1965. Wound healing and collagen formation. V. Quantitative electron microscope radioautographic observations of proline-^3H utilization by fibroblasts. *J. Cell Biol.* **27:**83.
58. Roth, T. F., and K. R. Porter. 1964. Yolk protein uptake in the oocyte of the mosquito *Aedes aegypti-L. J. Cell Biol.* **20:**313.
59. Salpeter, M. M. 1968. ^3H-proline incorporation into cartilage: EM autoradiographic observations. *J. Morphol.* **124:**387.
60. Sheldon, H., and F. B. Kimball. 1962. Studies on cartilage. III. The occurrence of collagen within vacuoles of the Golgi apparatus. *J. Cell Biol.* **12:**599.
61. Spiro, R. G. 1970. The carbohydrate of collagens. *In* Chemistry and Molecular Biology of the Intercellular Matrix. E. A. Balazs, editor. Academic Press, Inc., New York. 1.
62. Stack, M. V. 1955. The chemical nature of the organic matrix of bone, dentin and enamel. *Ann. N. Y. Acad. Sci.* **60:**585.
63. Stark, M., A. Lenaers, C. M. Lapiere, and K. Kühn. 1971. Electronoptical studies of procollagen from the skin of dermatosparaxic calves. *FEBS (Fed. Eur. Biochem. Soc.) Lett.* **18:**225.
64. Takuma, S. 1967. Ultrastructure of dentinogenesis. *In* Structure and Chemical Organization of Teeth. A. E. W. Miles, editor. Academic Press, Inc., New York. 1.
65. Takuma, S., and N. Nagai. 1971. Ultrastructure of rat odontoblasts in various stages of their development and maturation. *Arch. Oral Biol.* **16:**993.
66. Trelstad, R. L. 1971. Vacuoles in the embryonic chick corneal epithelium, an epithelium which produces collagen. *J. Cell Biol.* **48:**689.
67. Venable, J. H., and R. Coggeshall. 1965. A simplified lead citrate stain for use in electron microscopy. *J. Cell Biol.* **25:**407.
68. Vuust, J., and K. A. Piez. 1972. A kinetic study of collagen biosynthesis. *J. Biol. Chem.* **247:**856.
69. Warshawsky, H. 1972. The presence of atypical collagen fibrils in EDTA decalcified predentine and dentine of rat incisors. *Arch Oral Biol.* **17:**1745.
70. Warshawsky, H., and G. Moore. 1967. A technique for the fixation and decalcification

of rat incisors for electron microscopy. *J. Histochem. Cytochem.* **15**:542.

71. WATSON, M. L., and J. K. AVERY. 1954. The development of the hamster lower incisor as observed by electron microscopy. *Am. J. Anat.* **95**:109.
72. WEINSTOCK, A., and C. P. LEBLOND. 1971. Elaboration of the matrix glycoprotein of enamel by the secretory ameloblasts of the rat incisor as revealed by radioautography after galactose-^{3}H injection. *J. Cell Biol.* **51**:26.
73. WEINSTOCK, A., and R. W. YOUNG. 1972. Sulphate-^{35}S uptake by the Golgi apparatus of odontoblasts and the migration of label to the mineralization front of dentin. *J. Cell Biol.* **55**:276 a.
74. WEINSTOCK, A., M. WEINSTOCK, and C. P. LEBLOND. 1972. Autoradiographic detection of ^{3}H-fucose incorporation into glycoprotein by odontoblasts and its deposition at the site of the calcification front in dentin. *Calcif. Tissue Res.* **72**:181.
75. WEINSTOCK, M. 1972. Collagen formation–observations on its intracellular packaging and transport. *Z. Zellforsch. Mikrosk. Anat.* **129**:455.
76. WEINSTOCK, M., and C. P. LEBLOND. 1972. L'étapes de la synthèse du collagène. *Union Méd. Can.* **101**:2079.
77. WEINSTOCK, M., and C. P. LEBLOND. 1972. Elaboration of collagen by the odontoblasts of the rat incisor. *J. Cell Biol.* **55**(2, Pt.2): 277 a. (Abstr.).
78. WEINSTOCK, M., and C. P. LEBLOND. 1973. Radioautographic visualization of the deposition of a phosphoprotein at the mineralization front in the dentin of the rat incisor. *J. Cell Biol.* **56**:838.
79. WEINSTOCK, M. 1973. Elaboration of collagen precursors by osteoblasts in rat alveolar bone as visualized by electron microscope radioautography. Proceedings 31st Electron Microscopy Society of America Meeting. 346.
80. WELSH, R. A. 1966. Intracytoplasmic collagen formation in desmoid fibromatosis. *Am. J. Pathol.* **49**:515.
81. WHUR, P., A. HERSCOVICS, and C. P. LEBLOND. 1969. Radioautographic visualization of the incorporation of galactose-^{3}H and mannose-^{3}H by rat thyroids *in vitro* in relation to the stages of thyroglobulin synthesis. *J. Cell Biol.* **43**:289.